

Chapter 5

CW DYE LASERS

Leo Hollberg

*National Institute of Standards and Technology
(formerly National Bureau of Standards)
Boulder, Colorado*

1. INTRODUCTION	185
1.1. Overview of Characteristics	186
1.2. Brief History of the CW Dye Laser	186
1.3. Other Related Laser Systems	188
2. BASIC SYSTEM DESIGN	190
2.1. Example Systems	190
2.2. CW Output Powers	191
2.3. Dye Characteristics	192
2.4. Pump Sources	197
2.5. Resonator Design	198
3. EXTENDED TUNING	203
3.1. UV Generation	203
3.2. IR Generation by Difference-Frequency Mixing	205
4. LASER-FREQUENCY CONTROL	206
4.1. Frequency-Selective Elements	206
4.2. Frequency-Stabilization Methods	214
5. SPECTRAL CHARACTERISTICS	225
5.1. Amplitude Fluctuations	225
5.2. Frequency-Fluctuations	228
6. SUMMARY	232
PROBLEMS	232
REFERENCES	233

1. INTRODUCTION

The cw dye laser is a well-established tool of optical science. It plays the premier role as a source of tunable radiation in the visible and near-visible regions of the spectrum. This laser has a unique set of capabilities that include broad tunability, high power, and the potential for extremely high

* I gratefully acknowledge the helpful discussions and contributions made to this chapter by Dr. J.C. Bergquist, Dr. T.F. Johnston, Jr., Dr. J.L. Hall, Dr. S.L. Gilbert, and Dr. M. Young.

resolution. Because of these capabilities we overlook its high cost, sometimes complicated design, and the requirement of a high-power optical pump. No other optical source can provide a comparable combination of tunability, resolution, and power.

1.1. Overview of Characteristics

The most important attribute of the dye laser is its tunability, which gives the user access to essentially any wavelength in the visible and near-visible spectrum. The spectral range of ion-laser-pumped cw dye lasers is essentially complete coverage from 365 to 1000 nm. It is even possible to extend their cw tuning range by using nonlinear optical methods to generate wavelengths further into the ultraviolet and infrared. With the addition of these methods of nonlinear optical synthesis, the spectral range for complete coverage with cw radiation has been extended to 250 nm. Radiation at even shorter wavelengths has been generated for special applications. In addition nonlinear methods have been used to generate radiation in the 2–5 μm infrared region. This range of spectral coverage will certainly be extended in the future.

The power levels available from cw dye lasers are generally more than adequate for spectroscopic applications. The output power of cw dye lasers varies with the type of dye, but typical cw systems produce between .1 and 1 watt of output power. As with most things, there are some applications with almost unlimited demand for power. Special high-power cw-dye-laser systems have been developed that can produce tens of watts of tunable visible radiation.

With broad tuning ranges and narrow linewidths, single-mode cw dye lasers can provide an impressively large number of resolution elements. For example, a standard single-frequency dye laser (linewidth ≈ 1 MHz) operating with rhodamine 6G dye (tuning range ≈ 100 nm or $\approx 10^{14}$ Hz) is capable of resolving $\approx 10^8$ spectral elements across its tuning curve. If we considered one of the special high-resolution lasers that have been demonstrated (linewidths less than 1 kHz) the number of resolution elements is $\approx 10^{11}$, probably more than any application can actually use and certainly one of the highest of any electromagnetic source.

1.2. Brief History of the CW Dye Laser

Historically, the development of the cw dye laser was an outgrowth of research into the photophysics of dye-laser action in pulsed dye lasers (Schäfer *et al.*, 1966; Snavely and Schäfer, 1969). The first flashlamp-pumped dye lasers were developed in 1967 (Schmidt and Schäfer 1967; Sorokin and Lankard, 1967), just one year after the first successful pulsed

dye lasers, which were achieved using ruby lasers as the pump source (Sorokin and Lankard, 1966; Spaeth and Bortfeld, 1966; Stepanov *et al.* 1967). With flashlamp pumping, sufficient population inversion could be attained with surprisingly long output-pulse lengths. The pulse lengths were longer than expected because the trapping of molecular excitation in the unwanted triplet states was less probable than expected. The other important contribution that allowed cw operation was the development of a system to flow the dye rapidly through the pumping region in order to reduce the optical inhomogeneities induced in the dye by heating from the cw pump laser. In 1970 Peterson *et al.* (1970) demonstrated the first cw lasing of an organic dye. That laser used the dye, rhodamine 6G, with an argon-ion laser as the pump. Two decades later, the combination of the argon-ion laser and the rhodamine 6G dye is the most common, and in some ways, the best cw dye-laser system that exists.

That first cw dye laser appears extremely simple, but the design is very clever in solving some of the serious technical problems. Figure 5.1 is a simplified diagram of the type of laser design that was used in that first successful demonstration of a cw dye laser. This laser has the dye flowing between two dichroic mirrors that form the laser resonator as well as part of the containment cell for the dye. The argon-ion laser pumping beam was injected collinearly through one of the dichroic mirrors. The Peterson *et al.* (1970) laser of this type produced an output power of 30 mW in a spectral width of 3 nm when pumped with 1 W of 514-nm (argon ion) laser light. We can get some idea of the technological evolution of dye lasers by

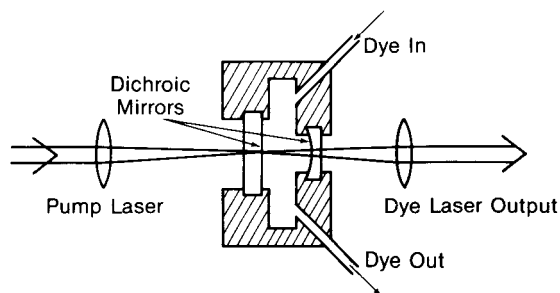


Fig. 5.1 Cross section of the type of dye laser used for the first successful cw operation. The two dichroic mirrors serve the dual role of containing the dye fluid and acting as the dye-laser resonator. The dichroic mirrors transmit the blue-green pump laser beam but are high reflectors for the reddish fluorescence from the dye. The pump-laser beam is derived from an Ar^+ laser. A lens is used to focus the pump beam into the dye cell at the dye-laser resonator waist which is on the flat dichroic mirror. The dye flows rapidly through the cell to remove the excess heat and triplet state population. With this type of laser Peterson *et al.* (1970) achieved ≈ 30 mW of cw dye-laser output power at 597 nm when the laser was pumped with ≈ 1 W of 514-nm light.

comparing these results with the performance characteristics of modern lasers, which can produce 1 W of output in a spectral width of about 10^{-6} nm (≈ 1 MHz) with a pump power of 6 W. More detailed discussion of the early cw dye lasers can be found in Tuccio and Strome (1972).

Development of the cw dye laser since 1970 has been extensive and continues in many labs around the world today. As in most technologies, progress in the development of the cw dye laser has involved a gradual improvement in the design of each of its components, combined with a few important discoveries that have significantly altered the basic system. The important achievements will be discussed in later sections, but it is useful to have some historical perspective of the development. One of the important developments that improved the performance of the dye laser was the introduction in 1972 (Runge and Rosenberg, 1972) of the jet-stream dye-circulation system, which gave more reliable high-power operation. About that same time techniques were developed that allowed frequency stabilization of these lasers and thus greatly enhanced their spectral resolving power (Barger *et al.*, 1973, 1975; Liberman and Pinard, 1973; Schröder *et al.*, 1973, 1975; Wu *et al.*, 1974, Hall and Lee, 1976b). The widespread use of traveling-wave ring lasers started in the late 70s and improved both the spectral characteristics and the power output from the cw dye lasers (Schröder *et al.*, 1977; Jarret and Young, 1979; Johnston *et al.*, 1982). The incorporation of computer control has provided automatic long-range tuning and enhanced data-collection capabilities (Marshall *et al.*, 1980; Williams *et al.*, 1983; Clark *et al.*, 1986). In addition to the continual improvement of laser dyes the '80s have seen the application nonlinear optical techniques that extended the spectral coverage that was possible with cw lasers into the UV and IR regions (Blit *et al.*, 1977, 1978; Couillaud, 1981; Couillaud *et al.*, 1982; Bergquist *et al.*, 1982; Hemmati *et al.*, 1983; T. F. Johnston, Jr., 1987; T. Johnston, 1988; Pine, 1974, 1976; Oka, 1988).

1.3. Other Related Laser Systems

Dye lasers are often the only choice or the best choice of laser for a given application, particularly if it is necessary to tune to a specific wavelength. In the dye laser's region of operation, only a few laser sources are competitive and those are only in limited parts of the dye laser's spectral region. A few new tunable lasers are beginning to threaten some of the traditional domains of the dye laser. These include semiconductor, color-center, Ti-sapphire, alexandrite, and a few optically pumped solid-state lasers. Other nontunable lasers exist that oscillate in the visible and near-visible region of the spectrum; for example, the Kr-ion and Ar-ion lasers have many useful lasing lines, and the optically pumped dimer lasers (sodium,

lithium, iodine, etc.) have hundreds of lines, but the lines are relatively narrow and, even when combining all of these lasers, the actual fractional coverage of the available spectrum is small.

Semiconductor lasers are now available in some parts of the near-IR and red regions of the spectrum. As of the late 1980s, in comparison with dye lasers the semiconductor lasers generally have large linewidths and low powers. But the characteristics of semiconductor lasers are improving and their future looks quite bright.

The broad class of optically pumped lasers shares many of the characteristics of the cw dye laser—for example, color-center lasers (Mollenauer, 1985; Mollenauer and White, 1987). Two important, and relatively new optically pumped solid-state lasers are the Ti-sapphire laser (Schulz, 1988) and the LNA (Lanthanide hexa-aluminate) laser (Scheerer *et al.*, 1986). The designs of these lasers, as well as that of color center lasers, are very similar to the designs of cw dye lasers. The Ti-sapphire laser is an interesting example of a laser competing for some of the domain dominated by the dye laser (Ti-sapphire tuning range $\approx 700\text{--}1000$ nm). These lasers use the same pumping source and essentially the same cavity design, but they have the dye medium replaced by a solid-state material. Most of the design features discussed here for dye lasers apply equally well to other optically pumped lasers. True, some types of lasers produce higher power, and some yield higher spectral purity, but the dye laser combines both of these traits with broad tunability and the ability to change dyes for even broader spectral coverage.

This chapter is not intended to be a comprehensive review of cw dye lasers but rather a description of the basic principles of some common cw dye lasers. Keep in mind that the descriptions are simply examples and the possible variations and extensions are large and often unexplored. This material is but a glimpse at the field from one perspective, where I have additionally chosen to cover in more detail those aspects that have been neglected in other sources, and to give less emphasis to material that is covered well elsewhere. Effort is made to give reference to other sources of material on cw dye lasers but the reference list is not complete. It is rather a place to start for further study. In this light it is important to note some of the review articles and books that are particularly relevant to the subject of cw dye lasers, including Shank (1975), Snively (1977), Schäfer (1977), Peterson (1979), and Mollenauer and White (1987). Of paramount interest is the excellent article by T. F. Johnston (1987) which is a review of dye lasers. Applications of dye lasers are discussed by Hänsch (1976) and Hall (1978). In addition, a great deal of useful information about the design and characteristics of cw dye lasers can be obtained from the instruction manuals of commercial laser systems.

2. BASIC SYSTEM DESIGN

2.1. Example Systems

The years since 1970 have seen the development of a large number of cw dye-laser designs. Two examples of dye-laser systems that have seen widespread use are the three-mirror folded-linear cavity and the four-mirror unidirectional-ring cavity. These systems are diagrammed in Fig. 5.2. We see some features that are common to both designs; for example, both use

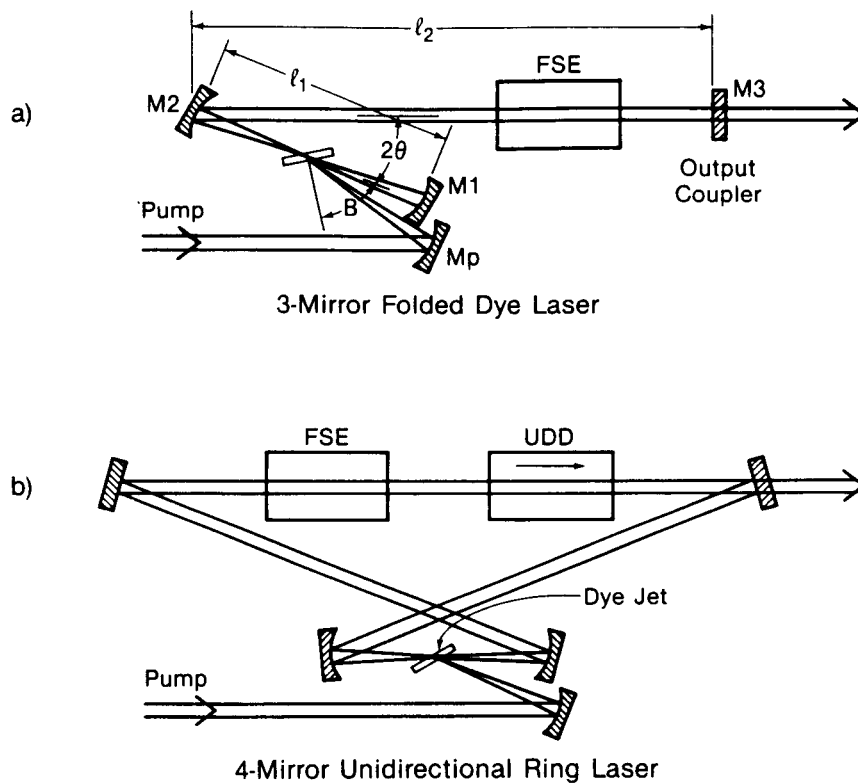


Fig. 5.2 Two popular cw dye-laser resonator configurations. The standing wave three-mirror resonator shown in (a) has a folded geometry with two short-radius curved mirrors (M_1 and M_2) and a flat output coupler, M_3 . The curved pump mirror, M_p , focuses pump beam on the dye jet, which is placed between M_1 and M_2 at the waist of the dye-laser resonator. FSE represents any frequency-selective elements that might be used inside the laser's resonator. In (b), another flat mirror has been added and the resonator is transformed into a figure-8-shaped ring. This resonator also has a unidirectional device, which ensures that the laser oscillates as a traveling wave, propagating in only one direction around the ring.

a free-flowing jet stream for the dye gain medium and a tightly focused ion-laser beam for the pump source. The two mirrors with short radii of curvature, which surround the dye jet, match the dye-laser cavity mode to the small pump spot. This strongly pumped region of the dye provides a high gain over a very short interaction length. The high gain allows flexibility in designing the other parts of the dye-laser resonator. The remaining components of these two resonators are chosen for specific attributes or applications and many variations of these basic systems are found. The frequency-selective elements, FSE, and the unidirectional device, UDD, in the ring laser, indicated schematically in Fig. 5.2, are components that control the frequency and lasing direction, respectively, and will be discussed in detail in a later section.

Some of the early cw dye-laser designs (which have not survived the test of time) used glass cells to contain the gain medium. In almost all modern cw systems the dye cells have been replaced by free-flowing dye jets. The introduction of the dye jet (Runge and Rosenberg, 1972) and its subsequent development (for example, Harri *et al.*, 1982) has been a major contribution to the success of the cw dye laser. The jets do not have the problem of the pump laser burning the dye on the cell windows. Also, much higher output powers can be obtained with dye jets, rather than cells, because more rapid flow rates are possible. Dye-cell lasers could have some advantage in low-power applications because they might have less frequency noise than the high-power dye-jet lasers. But in general the problems outweigh the advantages of the dye cells.

2.2. CW Output Powers

In the beginning it is useful to have a rough idea of the performance characteristics that can be expected from a modern cw dye laser. Curves for laser output power as a function of laser wavelength are shown in Fig. 5.3. These outstanding results are obtained for single-frequency cw-laser oscillation using a number of dyes, pump-laser lines, and changes of laser optics. One of the important things to notice here is that it is possible to have reasonably high output powers and single-frequency operation anywhere in the visible and near-visible spectrum (in fact from about 365 to 1000 nm). The broad spectral coverage demonstrates the versatility of the dye laser. With different ion-laser pump sources and 11 different dyes it is possible to generate high-intensity, coherent radiation with powers of up to several watts. In exceptional cases output powers as high as 33 W cw have been obtained from dye lasers (Anliker *et al.*, 1977).

The portion of the spectrum covered by the cw dye laser extends for more than an octave. The requirement of a large number of dyes is usually

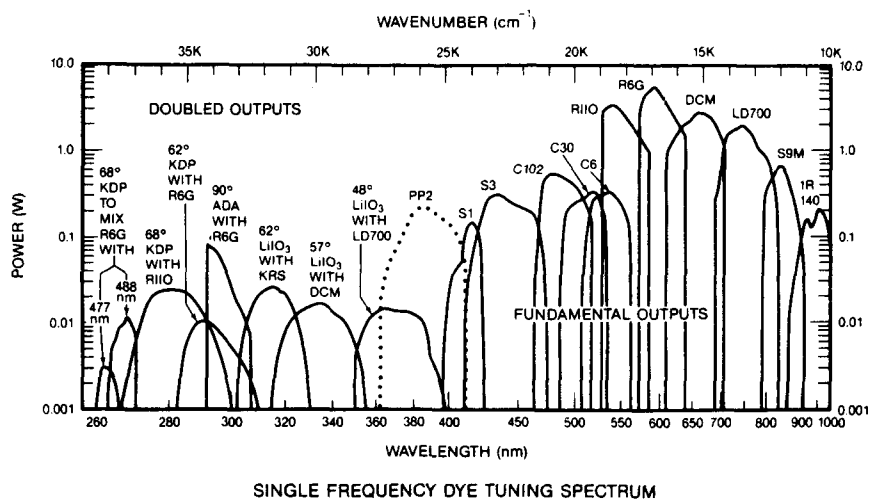


Fig. 5.3 Tuning curves of single-frequency dye-laser radiation, including frequency-doubled and sum frequency mixed outputs. The vertical axis is single-frequency power output displayed as a function of wavelength. The direct dye-laser output spans the spectral region from the blue end of the dye PP2 at ≈ 365 nm to the red end of the dye IR 140 at $\approx 1 \mu\text{m}$. The outputs from the intracavity frequency doubled radiation extends from ≈ 395 to 270 nm. The two curves at the extreme blue and end show the single-frequency power obtained by intracavity sum-frequency-mixing the R6G dye laser radiation with argon-ion laser lines at 488 and 477 nm. These curves are taken with permission from Johnston, T. F. (1987) and have been modified slightly to include the results from Johnston, T. (1988) for the dye PP2 (polyphenyl 2).

not a problem for most applications because spectroscopic studies usually have spectral windows that are easily covered by one dye. In fact, with the high resolution (approximately one MHz) of a single-frequency dye laser, there is often more spectroscopic resolution than is needed. Most of the UV outputs indicated in this figure (260–400 nm) are generated by using the strong visible dye-laser outputs and nonlinear optical-mixing methods.

2.3. Dye Characteristics

2.3.1. Absorption and Emission Spectra

The basic design of the cw dye laser is naturally constrained in fundamental ways by the photophysics and chemistry of the dye molecules. In Fig. 5.4 we see the representative absorption and emission spectra of a common laser dye. One of the important things to notice here is that the emission band is lower in frequency (red shifted) and is nearly the mirror image of the absorption band. In addition both the absorption and emission spectra are broadband features without sharp lines, indicative of a multitude of broadened mechanisms and overlapping energy levels. This is

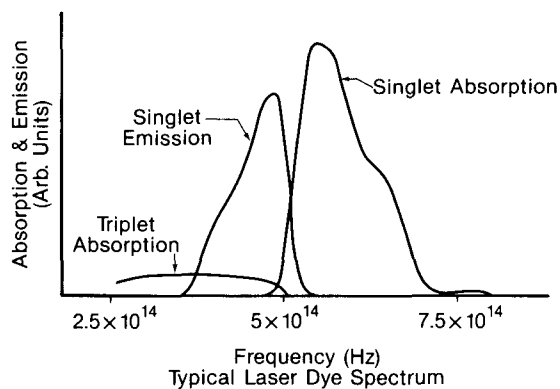


Fig. 5.4 Representation of typical absorption and emission spectra of a laser dye. The singlet emission spectrum is to the red and nearly the mirror image of the singlet absorption spectrum. Triplet absorption is smaller and typically extends even farther to the red than the singlet emission spectrum.

characteristic of large organic molecules in the liquid state and is depicted by a plausible energy-level diagram shown in Fig. 5.5. Here we see two manifolds of states, the singlets and the triplets, as designated by the net

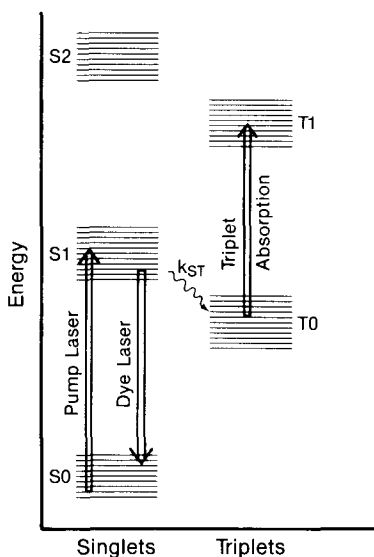


Fig. 5.5 Schematic picture of the energy levels of a generic laser dye, showing the singlet and triplet manifolds of states. The double lined arrows represent the optical redistribution of excitation by the pump laser, by the dye-laser emission (and dye fluorescence), and by triplet-state absorption. The arrow labeled k_{st} represents the transfer of excitation from the singlet to the triplet manifolds.

electronic spin. The transitions from the singlet manifold to the triplet manifold have low probability because they require an electron spin flip. The large organic-dye molecules have many internal degrees of freedom (vibration and rotation) that give rise to broad overlapping energy levels and spectra. The transfer of excitation within these energy bands can be very rapid, with typical time scales on the order of a picosecond. This energy transfer within a band is much faster than the spontaneous decay rates for interband transitions which have nanosecond time scales.

For laser oscillation the dye molecule's absorption band is excited by the intense pump laser from the lower part of the ground state, S0, to higher energy regions of the first excited singlet state S1 (Fig. 5.5). This excitation energy is then rapidly redistributed within the S1 state and reappears predominantly as fluorescence photons as the molecule decays by an electric-dipole transition from the S1 state to the S0 state. This transition in the singlet manifold from the first excited-electronic state S1 to the upper regions of the ground state S0 is the lasing transition. It is obviously advantageous to have efficient conversion of the pump photons into fluorescence photons and to avoid the loss of the pump energy to other channels. The primary loss mechanism (indicated on Fig. 5.5) is the transition from the S1 state in the singlet manifold to the T0 state in the triplet manifold. This excitation, which reaches the triplet states, is detrimental for two reasons. First, it is a loss of available energy from the lasing singlet system. Second, the population in the T1 state can absorb photons by making transitions to higher levels in the triplet manifold, thereby creating additional loss for the laser system. The characteristic time scale for the transfer of population from the S1 state to the T0 state is typically 100 ns. This needs to be compared with the time scales for other processes that affect the excited-state population. These are the fluorescence lifetime for the S1–S0 transition (typically a few nanoseconds) and the time scale for transfer of population within the S1 state (typically one ps). With the good laser dyes available today, the conversion efficiency, in terms of fluorescence photons (S1 decays to S0) for pump photons, is in the range of 0.8 to 1.0. Note that this efficiency is not the energy-conversion efficiency because of the difference in color between the pump and fluorescence photons.

2.3.2. Dye-Laser Gain and Threshold

Following the treatments of Shank (1975) and Johnston (1987) and making some simplifying assumptions that ignore the actual spatial distribution of the pump and the dye laser intensities we can write the small-signal gain of the laser as

$$\alpha_0 \ell = \frac{N \ell \beta_p I_p (\sigma_e - k_{st} \tau \sigma_t - \sigma_a)}{h \nu_p + \beta_p I_p (1 + k_{st} \tau)}. \quad (5.1)$$

Here, $\beta_p = \sigma_p \tau \phi$, h is Planck's constant, ν_p is the pump frequency, τ is the spontaneous emission lifetime and ϕ is fluorescence efficiency. This efficiency is the ratio of the fluorescence decay rate to the total decay rate for the S1 state and is usually near 1 for most good laser dyes. The quantities σ_p , σ_a , and σ_e are the singlet pumping, absorption, and emission cross sections, respectively. N is the density of dye molecules, ℓ is the dye-jet interaction length, and I_p is the intensity of the pump laser. The factor k_{st} is the rate of transfer of population from the singlet to the triplet manifold and multiplies the triplet absorption cross section σ_t . Above threshold the dye laser will show laser-intensity-dependent saturation as is usual for a homogeneously broadened system; that is,

$$\alpha \ell = \frac{\alpha_0 \ell}{1 + I_e/I_s}. \quad (5.2)$$

The saturation intensity I_s is a characteristic of the dye and is a function of the pump intensity and limits the gain as the dye laser intensity I_e increases.

For example, we can make the reasonable assumptions that the loss terms σ_a (which represents absorption of the dye-laser radiation by the dye itself) and k_{st} (the singlet-to-triplet transfer rate) are small enough to be ignored. Then Eq. (5.1) becomes

$$\alpha_0 \ell = \frac{N \ell \sigma_p I_p \tau \sigma_e}{h \nu_p + \sigma_p I_p \tau \phi}. \quad (5.3)$$

The pump intensity at threshold can be estimated from Eq. (5.3) by equating the gain to the resonator losses. We shall represent the total resonator loss as T , which is the sum of the output coupling transmission and the actual scattering and absorption losses. The threshold pump intensity is then

$$I_{p,\text{th}} = \left(\frac{h \nu_p}{\sigma_p \tau \phi} \right) \left(\frac{T}{N \ell \sigma_e - T} \right). \quad (5.4)$$

The optimum transmittance of the output coupler for most cw dye lasers ranges from 1 to 15% and is almost always the dominant loss term for the laser resonator.

By using typical values for the dye rhodamine 6G and the parameters in Eq. (5.4), we can estimate the minimum required pump intensity for laser oscillation. For rhodamine 6G we expect $T \approx 15\%$, $\ell = .01$ cm, $N \approx 10^{18}$ cm⁻³, $\sigma_e = \sigma_p \approx 1 \times 10^{-16}$ cm², $\nu_p = 5.8 \times 10^{14}$ Hz, $\tau \approx 3$ ns, and $\phi \approx 1$. This gives a rough value for the pump intensity at threshold of $I_{p,\text{th}} \approx 2 \times 10^5$ W/cm². Such high intensities can be obtained continuously only at the focus of a strong pump laser. Actual operation of a cw dye laser will often be at pump intensities that are several times the threshold value.

In these simple considerations we have neglected many factors that strongly influence the gain and tuning characteristics of dye lasers. Two of the important omissions here are the spatial dependence of the pump and dye laser modes (Tuccio, 1971), and the wavelength dependence of the gain and loss cross sections. A more complete discussion of dye-laser gain can be found in Chapters 1, 3, and 7 as well as in articles by Peterson *et al.* (1971), Peterson (1979), Danielmeyer (1971), Snavely (1977), Shank (1975), and Kuhlke and Dietel (1977).

Two conclusions that we can glean from this calculation are that with practical pump powers the useful gain in laser dyes will be achieved in a very small active region and that the gain will be large. High gain is an asset in that it allows design flexibility because the laser is relatively insensitive to small amounts of extra loss. This, in part, is the reason that there are so many different dye-laser designs. Almost anything works if you have enough gain. Thus dye lasers can be designed with characteristics optimized for specific applications. Even though high pump powers are often needed to reach threshold with dye lasers, the high slope efficiencies that are possible result in laser-conversion efficiencies from pump power to dye-laser power that can be quite acceptable (even as high as 50% in some cases). However, at the highest pump powers the effects of gain saturation and dye heating limit the ultimate powers that are achieved.

2.3.3. Broadening—Homogeneous versus Inhomogeneous

The most important aspect of the gain of organic dyes is that it is spectrally broad. The processes that determine the spectral width are categorized according to whether they are homogeneous or inhomogeneous. Operationally there are important distinctions between the two classes of broadening. Homogeneous broadening means that all of the gain medium can contribute power to the oscillating laser mode. In contrast, for inhomogeneously broadened systems, only a fraction of the total gain is available for a specific oscillating mode. The physics of a specific broadening mechanism will determine whether the broadening is homogeneous or inhomogeneous. In the case of homogeneous broadening, all of the excited molecules (or atoms, or excited carriers, etc.) are effectively equivalent and can emit radiation at any frequency within the fluorescence bandwidth. In inhomogeneously broadened systems, on the other hand, the emission spectrum of a specific group of excited molecules is different from the emission spectrum of the system as a whole. When the broadening is inhomogeneous the molecules can be divided into groups that have distinct absorption and emission spectra. The Doppler shift is the best example of inhomogeneous broadening; atoms with different velocities have different emission spectra and hence contribute gain to a laser

oscillator at different frequencies. On the other hand, the broadening due to collisions (for example, in a dense liquid) is homogeneous broadening.

The homogeneous broadening of the gain of organic dyes is both a blessing and a curse. It is a blessing in the sense that most of the available gain can be used for a single oscillation frequency and because the broad emission spectrum provides the laser's tunability. It is a curse because the broad spectral width means that the excited-state lifetime is short and hence intense pump powers are required in order to achieve sufficient population inversion for laser oscillation.

2.3.4. Dye Lifetimes

An annoying characteristic of organic dyes is that the dyes have limited productive lifetimes. (Unfortunately this is also the case for laser scientists!) The factors that limit the lifetime of laser dyes are thought to be the chemical and photochemical degradation of the dye in solution. The lifetime of the gain of a dye is often specified in terms of watt-hours, based on empirical data. This power-lifetime product is a measure of the pump-laser energy that has been used to excite the dye. Thus the degradation must be at least in part due to thermally activated chemistry (resulting from the pump-laser heating of the dye) and/or actual laser-induced photochemistry in the dye solution. The chemistry of the dyes can be quite complicated as is evidenced by the fact that the lifetime of the dyes' gain can even be affected by the type of metal plumbing components used in the dye-circulating system. The lifetimes of the typical cw dyes range from $\approx 75 \text{ W} \cdot \text{hr}$ (coumarin 480) to several $1000 \text{ W} \cdot \text{hr}$ (Rh6G). Obviously the predicted lifetimes are estimates of typical performance and cannot be depended upon without further specification of the conditions. For example, the lifetimes usually assume a typical dye-pumping system with approximately one liter of dye solution.

2.4. Pump Sources

We require strong, broad fluorescence from the dye for broadly tunable cw laser operation. This in turn requires an intense optical-pump source tuned to some part of the absorption band of the dye. Incoherent optical pumping of a cw dye laser to threshold has been demonstrated by Thiel *et al.* (1987) using high-pressure arc lamps; but in order to have sufficient intensity for a practical system, the pump sources are almost always cw ion-lasers. In practice, we are presently limited to the argon and krypton-ion lasers. The obvious reason is that they are the only cw lasers that can produce high enough power ($>4 \text{ W}$, say) in a good single-spatial mode and in the visible or UV region of the spectrum. Recall that the dye's emission band is to

Table 5-1
Powers Available from High-Power Ion Lasers

	Wavelength (nm)	Power (W)
Argon ion	528.7	1.5
	514.5	10.0
	501.7	1.5
	496.5	2.5
	488.0	7.0
	476.5	2.8
	472.7	1.2
	465.8	0.75
	457.9	1.4
	454.5	1.0
	Multiline visible	18-25
	Multiline UV	5.0
	351.1-385.8	3.0
	333.6-363.8	5.0
275.4-305.5	0.6	
Krypton ion	Multiline	—
	752.5-799.3	1.6
	647.1-676.4	4.6
	520.8-568.2	3.6
	468.0-530.9	2.5
	406.7-422.6	1.3
	337.5-365.4	2.0

the red of the absorption band; this means that for visible dye lasers we need strong blue and UV pump lasers. As of 1989, we are stuck with the very inefficient high-power ion-lasers for dye-laser pumping. Some of the strongest lines that are available from high-power ion-lasers are listed in Table 5-1. To be useful as a laser dye, a compounds-absorption band must overlap one of these strong ion laser lines. Other pump sources are certainly possible. For example, dye lasers can be pumped with a HeNe laser at 633 nm (Runge and Rosenberg 1972; Thiel *et al.*, 1986) and also the future holds promise for pumping with high-power green light (532 nm) obtained from frequency doubling the output of cw YAG lasers. There has also been some progress in designing dye lasers that could be pumped with concentrated solar radiation (Lee *et al.*, 1988).

2.5. Resonator Design

A good way to understand the performance characteristics of modern cw dye lasers is to study an example laser that is typical of modern designs.

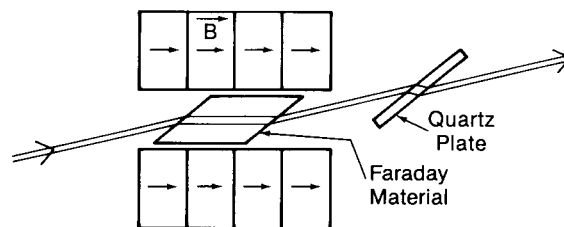
pump radiation from ion laser is focused by the pump mirror to a small spot size ($w_0 \approx 15 \mu\text{m}$) on the flowing jet of dye. Because of the heat produced in the dye by the focused pump laser and because of triplet-state trapping, it is necessary to have the dye molecules traverse the pump spot very rapidly, where “rapidly” in this case is determined by the heating rate and by the rate of transfer of excitation to the triplet state (typically about 1×10^{-7} s). To avoid significant loss into the triplet manifold the dye fluid needs to traverse the pumping region at a velocity of about 10 m/s. Usually the dye jet is a nearly rectangular ribbon with a cross section of 0.1 by 3 mm and is oriented at Brewster’s angle (to minimize reflection loss) relative to the laser-cavity mode and near Brewster’s angle to the pump beam. The laser mode passes through the thin dimension of the dye jet. The concentration of the organic dye in the transporting fluid is chosen to be high enough that the dye absorbs about 85% of incident pump radiation.

2.5.1. *Spatial Hole Burning*

The first question we need to address about the design of the laser cavity is why have we abandoned the linear three-mirror cavity of Fig. 5.2 in favor of the ring resonator of Fig. 5.6. The problem with the linear cavity is spatial hole burning. This is easily understood by thinking about the longitudinal mode structure of a linear dye-laser cavity. The dye laser’s oscillating mode traverses the dye jet twice, in opposite directions; this sets up a standing wave field in the gain medium. The standing wave is a strong periodic spatial modulation of the laser intensity across the gain medium. Because of the intensity-dependence of stimulated emission, a single-frequency laser mode is only able to use the gain that is available where the field strength is high. But we recall that the pumping field is a traveling wave that provides gain throughout the jet. Thus gain at the nodes of the standing wave cannot be used by the single-mode oscillatory field. The laser can, and will, use this available gain by oscillating simultaneously at a different frequency so that the nodes of the new oscillating mode overlap the antinodes of the original mode. The effect of spatial hole burning is to cause the linear standing-wave cavity to oscillate with more than one frequency (longitudinal mode).

2.5.2. *Unidirectional Ring Laser*

The problem of spatial hole burning can be alleviated by designing a laser resonator that oscillates in a traveling wave rather than a standing wave. Both the effect of spatial hole burning and its solution have been known for quite some time (Tang *et al.*, 1963; Danielmeyer, 1971; Pike, 1974; Green *et al.*, 1973; Kuhlke and Dietel, 1977), but it was not until about 1977 (Schröder *et al.*, 1977) that the travelling-wave ring dye lasers



Unidirectional Device

Fig. 5.7 Cross-section diagram of a unidirectional device (optical diode). A stack of permanent magnets creates a strong magnetic field (a few kG) within its central bore which contains Faraday material. The quartz "rotate-back" plate uses optical activity to rotate the polarization of the laser field. Thus, the laser-propagation direction inside the quartz plate must be along the z-axis of the crystal. The configuration shown here is designed for minimum loss with both the Faraday material and the quartz plate oriented at Brewster's angle relative to the laser-propagation direction. For the beam propagating in the direction shown, the net rotation of the polarization is 0° , whereas the other direction has a net rotation of about 4° .

came into prominence (Jarrett and Young, 1979; Johnston *et al.*, 1982). An interesting discussion of using prisms to create ring resonators for dye lasers is given by Marowsky and Zaraga (1974).

To avoid lasing in both directions, the ring laser's cavity must have more loss for one of the two propagation directions. This increased loss for one direction is provided by a nonreciprocal loss element, depicted in Fig. 5.6 as an optical diode. This optical diode (or unidirectional device) provides the directionally specific loss by using the axial vector nature of magnetic fields. A typical unidirectional device is diagrammed in Fig. 5.7. The device works by rotating the polarization of the propagating laser mode for only one of the two propagation directions. The rotated polarization encounters extra loss in the remaining Brewster-angle elements of the ring cavity. The rotation is made nonreciprocal by the Faraday effect of a crystal or glass in a magnetic field (applied parallel to the direction of propagation of the laser mode). The direction of polarization rotation due to the Faraday effect is independent of the direction of propagation of the light through the material. This Faraday rotation can then be combined with a reciprocal polarization rotation to produce an optical diode that rotates the direction of polarization for a beam from one direction but has no net rotation for a beam from the other direction. The reciprocal rotation is easily obtained from the optical activity in a thin quartz plate. A small differential loss of about $\approx 0.5\%$ is sufficient for unidirectional operation of most ring dye lasers. This loss is achieved from a one-way polarization rotation of about 4° in a laser cavity that has six Brewster surfaces or more. The design criteria for unidirectional devices are discussed by Biraben (1979) and by Johnston and Proffitt (1980).

Unidirectional ring lasers with traveling wave fields have advantages over standing-wave lasers because of more efficient use of the available gain and better spectral characteristics. On the other hand, with ring lasers there is reduced gain per pass because the radiation field only traverses the gain medium once for each incidence on the output coupler. The net result is that with sufficient pump power the traveling-wave ring dye lasers can provide almost twice the single-mode output power of the standing-wave lasers. For this extra power and mode stability ring lasers have the disadvantage of slightly higher cavity loss because of the extra optical components. This means that the thresholds are typically higher for ring cavities. Some of the very low gain dyes actually work better in linear cavities because of their lower threshold.

From the gain arguments just given and knowledge of the pump powers that are available, we know that the gain medium will occupy a small volume (about 10^{-7} cm³). To optimally use the available gain the dye laser's spatial mode is approximately matched to the pump-laser spatial mode in the dye medium. "Approximately matched" here indicates that the optimal size of the pump and dye laser modes is actually a function of the saturation of the gain medium and is thus a weak function of the pump power (Snavely, 1977; Johnston, 1987). In practical cases, where the laser operates well above threshold, this dependence is weak and is usually not worth the trouble of readjusting the laser mode when the pump power is changed. We usually have a pump-laser spot size of about $w_0 = 15$ μ m, which is consistent with the available pump powers and the threshold intensity of the dye. We can then use Gaussian mode analysis to calculate the transverse mode structure for a laser resonator (Yariv, 1975; Siegman, 1986). This analysis can give us the information that is necessary to select the mirror spacings, orientations, and radii of curvature that will approximately match the dye-laser mode to the gain region.

2.5.3. Resonator Aberrations

Up to now we have naively assumed that the natural fundamental transverse mode structure of the dye laser is the round TEM₀₀ mode. But in fact the orientation of the curved mirrors in the laser cavity relative to the incidence angle of the laser beam alters the transverse structure of the TEM₀₀ mode. Having a laser beam incident on spherical mirrors at an angle other than normal incidence causes the beam to be aberrated by astigmatism and coma. The dye jet is also a source of astigmatism and coma because it intercepts the strongly focused Gaussian laser mode at an angle. These aberrations distort the laser mode from the desired TEM₀₀ mode, and this degrades the resonator's stability and reduces the laser's conversion efficiency. In most modern designs the astigmatism is compen-

sated by the appropriate choice of angles of the resonator's mode at the curved mirrors or by the addition of other optical elements that introduce an astigmatism of the opposite sign. It is even possible to simultaneously compensate for both astigmatism and coma. Details of the compensation methods can be found in Kogelnik *et al.* (1972), Johnston and Runge (1972), and Dunn and Ferguson (1977).

Using the geometry shown in Fig. 5.2a, we can follow the analysis of Kogelnik *et al.* (1972), and Mollenauer and White (1987) to calculate the astigmatism introduced by the two curved mirrors and the dye jet. The dye jet with thickness t is located between the two short-radius curved mirrors (M1, M2) and is tilted at Brewster's angle B relative to the beam-propagation direction. In this geometry there are two sources of astigmatism; the first is that due to the dye jet crossing the laser mode at an angle and the second due to the curved mirror M2 that is tilted at the angle θ relative to the laser-mode—propagation direction. Fortunately, the sign of the astigmatism is opposite for these two sources, and the angles can be chosen so that the mirror astigmatism cancels that of the jet. The condition for zero astigmatism is

$$f(\sin \theta)(\tan \theta) = t(n^2 - 1) \frac{\sqrt{n^2 + 1}}{n^4}, \quad (5.5)$$

where f is the focal length of mirror M2 and n is the index of refraction of the gain medium (Kogelnik *et al.*, 1972). Since the dye jets are quite thin (≈ 0.1 mm) and the mirrors have radii of about 5 cm, the angle θ must be small. These small angles are not always practical, so other methods have been used to compensate the astigmatism. These includes lenses or additional curved mirrors that are titled off normal incidence, a Brewster plate between the dye jet and the short-radius mirrors, and rhombi with Brewster-cut surfaces that are placed in an auxiliary beam waist in the laser cavity.

3. EXTENDED TUNING

3.1. UV Generation

Nonlinear optical methods can be used with dye lasers to extend the already broad tuning range of cw dye lasers. If we look back to Fig. 5.3 we see the UV-tuning curves that were obtained by T. F. Johnston (1987) and T. Johnston (1988) using a high-power single-mode cw dye laser. This cw single-frequency UV output is generated either by frequency doubling the output of the dye laser or by sum-frequency mixing the output of the dye

laser with the output of a single-frequency argon-ion laser. Using these methods, they have generated single-frequency cw UV radiation across the frequency range between 260 and 400 nm. The excellent UV powers obtained in these experiments were typically about 10 mW. Both the doubling and the frequency mixing were done inside the resonator of a ring dye laser. For the sum-frequency mixing experiments the two laser resonators were actually arranged to overlap at the nonlinear crystal. Thus the mixing occurred with buildup on both the input frequencies. Other systems have been developed to generate cw ultraviolet light in this frequency range and beyond (Frölich *et al.*, 1976; Blit *et al.*, 1977, 1978; Couillaud, 1981; Couillaud *et al.*, 1982; Marshall *et al.*, 1980; Bergquist *et al.*, 1982; Hemmati *et al.*, 1983). The transparency of the nonlinear crystals limits cw UV generation to wavelengths longer than approximately 160 nm. That is not the case for UV generation in atomic vapors. Four-wave mixing has been used in strontium vapor to generate ≈ 10 pW of broadband (≈ 6 GHz) cw UV radiation at 170 nm (Freeman *et al.*, 1978).

Noteworthy among these efforts to generate single-frequency cw UV radiation is the work of Bergquist and collaborators (Bergquist *et al.*, 1982; Hemmati *et al.*, 1983), who have combined the second harmonic of argon-ion laser radiation (fundamental = 514 nm) with tunable dye-laser radiation (≈ 792 nm) to generate UV radiation at 194 nm. Other colors could certainly be generated by these methods but the 194-nm radiation is of particular interest for high-resolution spectroscopy of Hg ions. Their system is diagrammed in Fig. 5.8. It serves as good example of the techniques and the 1980s state of the art for synthesizing single-frequency cw, UV radiation. Their system uses the nonlinear crystal KB5 (potassium pentaborate) to generate the sum frequency of 792- and 257-nm radiation. The 792 nm radiation comes from a cw ring dye laser (LD700 dye), and the 257 nm radiation is from the frequency-doubled 514 nm argon laser. One of the techniques they use to advantage is putting the nonlinear crystals in external ring buildup cavities. This enhances the optical power in the nonlinear crystals and avoids the problem of the crystal's loss in the laser resonator. A ring cavity containing a Brewster-cut ADP (ammonium dihydrogen phosphate) crystal is locked to and enhances the power of the 514 nm radiation by a factor of ≈ 33 . Thus 700 mW of 514 nm radiation generates about 30–40 mW of 257 nm radiation. Then, as shown in Fig. 5.8, they use two buildup cavities around the KB5 summing crystal; one ring cavity builds up the 792-nm radiation and the second ring resonator builds up the 257-nm radiation. Both these cavities have buildup factors of ≈ 15 . With input powers of ≈ 120 mW at 792 nm and ≈ 30 mW at 257 nm they obtain ≈ 20 μ W of cw single-frequency radiation at 194 nm. The output power at 194 nm is not limited by the availability of input powers

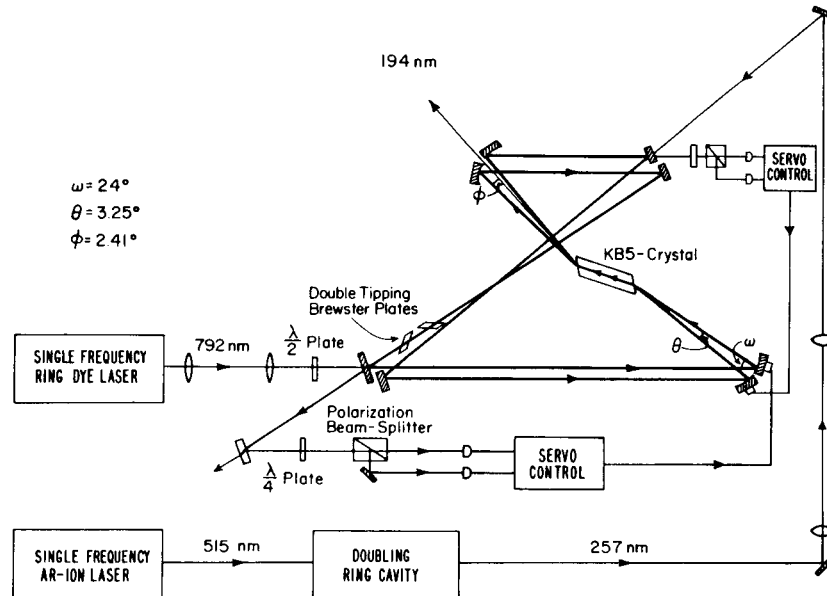


Fig. 5.8 Sum frequency generation of 194-nm radiation. This system, developed by Hemmati *et al.* (1983), and Bergquist (1989) uses the nonlinearity of the KB5 crystal to generate the sum frequency of 257- and 792-nm radiation. The power in both of these input beams is enhanced in ring buildup cavities whose waists intersect in the KB5 crystal. Servo-control loops (using the polarization lock method) keep the two buildup cavities locked to their respective input beams. The 194-nm radiation leaves the KB5 crystal at a slightly different angle and thus escapes from the two buildup cavities. The 792-nm input radiation comes from a frequency-stabilized ring dye laser, while the 257-nm is generated by frequency doubling the 514-nm radiation from a single-frequency argon-ion laser. The frequency doubling of the argon-ion laser radiation is done in a ring buildup cavity that is similar to the two used around the KB5 crystal shown here. With input powers of ≈ 30 mW at 257 nm and 120 mW at 792 nm, this system generates up to $20 \mu\text{W}$ of single-frequency radiation at 194 nm. Unpublished figure reprinted with permission from Bergquist (1989).

but rather by the effects of thermal blooming due to nonuniform optical heating of the KB5 crystal. Another important technique of nonlinear optics that is used in this system is electronic servo-control systems to maintain the resonance condition for the buildup cavities (see section 4 on laser frequency control).

3.2. IR Generation by Difference-Frequency Mixing

The useful tuning range of dye lasers can be similarly extended into the infrared by difference-frequency mixing (Pine, 1974, 1976; Oka, 1988). The technique is analogous to the sum-frequency generation, but now the

crystal's nonlinearity is used to generate the difference frequency between an ion-laser beam and a tunable cw dye laser. Using LiNbO_3 as the nonlinear crystal Pine (1974, 1976) has demonstrated that one can produce narrowband (≈ 15 -MHz linewidth) radiation with wavelengths in the range of 2.2 to 4.2 microns and with power levels of a few microwatts. The tuning range can be extended by using other nonlinear crystals such as lithium iodate (Oka, 1988). Somewhat higher power levels can also be achieved.

One problem with describing the late 1980s state of the art is that there is a tendency to report the best performances rather than what is typically achieved. The output-power curves shown in Fig. 5.3 are an example of what is possible with an optimized dye laser with very powerful pump lasers. The performance that you should expect from a typical commercial dye laser system is probably a factor of two less power than shown there. Nevertheless the record performances are always interesting, because research continues to expand our possibilities and the best results today are indicative of the tools of the future. In addition, the extreme limits are often dominated by new and interesting science waiting to be explored.

4. LASER-FREQUENCY CONTROL

High-resolution dye lasers are common laboratory tools today because of early research efforts in laser frequency control. The broad bandwidth of the gain medium, combined with the mechanical instabilities of the rapidly flowing dye jet, conspire to make frequency selection and stabilization a challenge. Nonetheless, the technology required to control the frequency of dye lasers has been developed. Many years ago, Soffer and McFarland (1967) demonstrated that the wide bandwidth of pulsed dye lasers could be compressed to a relatively narrow bandwidth by inserting an optical grating inside the cavity. In addition to reducing the laser's linewidth, the frequency selectivity of the grating allowed the laser's wavelength to be tuned. This demonstration of spectral compression, as well as more recent techniques, takes advantage of the homogeneous broadening of the dye laser gain to produce a narrower spectral linewidth without sacrificing output power.

4.1. Frequency-Selective Elements

The laser's oscillation frequency can also be controlled by providing frequency-selective loss inside the resonator. To achieve this frequency-selective loss, we have freedom to control both the spatial and polarization boundary conditions of the resonator. Dispersive optical elements that create boundary conditions for the oscillating mode provide the appropri-

ate frequency-selective loss. The dispersion can come from interferometry, which is solely wavelength-selective, or it can be provided by polarization-sensitive elements which act on the vector nature of the optical field. Some of the dispersive elements that have been used to control the frequency of cw dye lasers include gratings, prisms, birefringent filters, and Fabry-Perot etalons, as well as Michelson, Fox-Smith, and Mach-Zehnder interferometers (Smith, 1972).

Usually the addition of one frequency-selective element into a dye laser's cavity is not sufficient to uniquely determine the laser's oscillation frequency. The conventional technique to achieve mode-stable single-frequency operation is to use a hierarchy of frequency-selective elements inside the laser's cavity. Most single-mode lasers use three separate levels of frequency selectivity to force the laser to oscillate on a specific longitudinal mode of the laser's cavity. Lacking this hierarchy of frequency selectivity, the laser may oscillate with many modes, or it may oscillate with a single mode that is unstable to small perturbations and jump from mode to mode as a function of time.

Due to the homogeneous broadening of the gain, once the laser starts to oscillate on a specific mode, this mode quickly depletes the gain that is otherwise available for the other longitudinal modes. In a traveling-wave ring dye laser the homogeneous broadening causes strong mode competition, which is usually enough to ensure that the laser will oscillate on a single longitudinal mode. Unfortunately, without frequency selectivity in the cavity, the oscillating mode is unstable to small perturbations and will change in time. Thus even though the laser oscillates on a single mode, additional frequency-selective elements inside the cavity are necessary to select a particular frequency.

A typical hierarchy of frequency-selective elements might start on the least selective end with a birefringent filter, which typically has a half-power bandwidth in the laser resonator of about 1800 GHz (60 cm^{-1}). This is usually followed by two etalons, with progressively higher resolution; for example, a thin etalon with a free spectral range (FSR) of 200 GHz and a finesse of ≈ 3 , then a thick etalon with a FSR of 10 GHz and again a finesse of ≈ 3 . The overlap of the transmittance peaks of the three frequency-selective elements provides a net transmittance bandwidth that is narrow enough to uniquely determine a single mode for laser oscillation. The role of the various frequency-selective elements can be seen in Fig. 5.9, which shows the transmission functions of these elements overlaid with the laser longitudinal mode structure. The resolving powers of the three levels of frequency-selectivity are chosen so that the resolution of one level is sufficient to select a unique resolution element of the next higher level of selectivity. Thus, the birefringent filter has enough resolution to select a

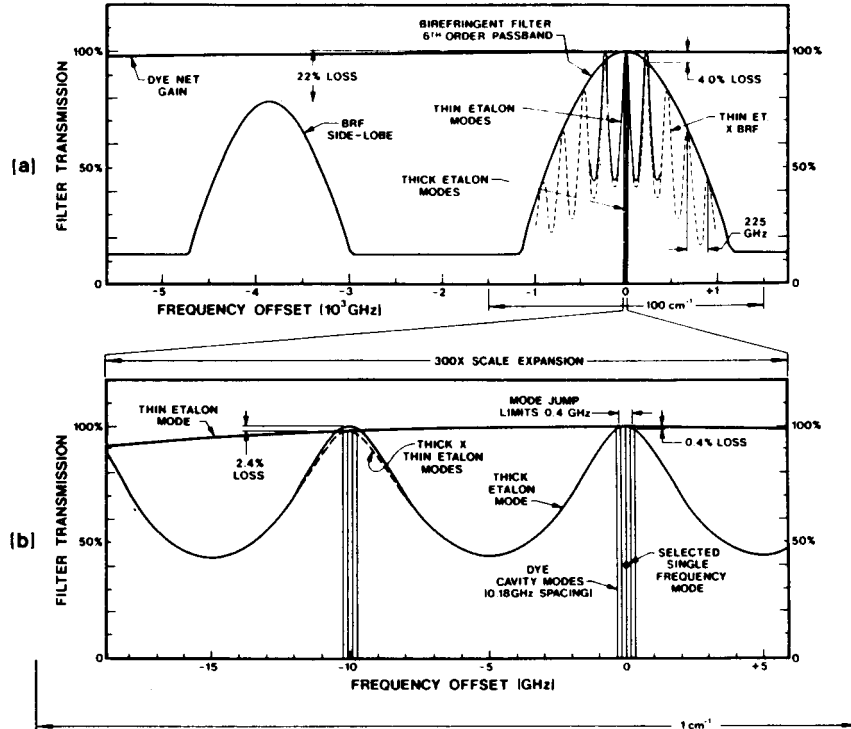


Fig. 5.9 Filter transmission functions of the various frequency-selective elements of a single-frequency dye laser. The traces show the bandpasses of the frequency-selective elements relative to the dye gain curve and the laser's cavity-mode structure. The upper half of the figure has a broad spectral range and shows the birefringent filter and thin-etalon transmission functions. The lower half of the figure shows the thick etalon's transmission function relative to the longitudinal mode spacing (c/L with L = cavity round-trip length) of the laser cavity. Also indicated are the losses created for radiation away from the central transmission peaks. This figure is reprinted with permission from Coherent Inc. and Johnston, T. F. (1987).

specific thin-etalon mode, the thin-etalon selects a specific thick-etalon mode, and the thick etalon has enough resolution to select a specific longitudinal mode of the laser cavity. For the system to work in an optimum way, the bandpasses of these filters need to be at least roughly centered on a specific cavity mode. Figure 5.6 is an example of a single-frequency dye laser with a slightly different hierarchy of frequency-selective elements, in this case a prism and two etalons.

The frequency stability of such single-frequency lasers is now determined by the mechanical stability of the optical elements, the gain

medium, and the resonator's superstructure. We shall see in the spectral characteristics section (5.2) that "single frequency" is a bit optimistic, in that the spectral linewidth of single-mode lasers can still be substantial.

The birefringent filter is the most common coarse tuning element and is composed of quartz plates placed in the laser cavity inclined at Brewster's angle relative to the direction of propagation (Bloom, 1974; Bonarev and Kobtsev, 1986). The thickness of each plate in the filter is integrally related to the others (for example, 1:4:16 for a common three-plate birefringent filter). The quartz plates are cut with the optic axis parallel to the surface of the plates. The design of the birefringent filter for a laser follows the traditional Lyot filter design (Jenkins and White, 1957), with the important difference that the polarizers between the birefringent elements have been removed. The role of the polarizers is played by the Brewster-angle surfaces of the plates themselves and other Brewster surfaces in the cavity. The optical frequency selectivity of this filter results from the birefringence of the quartz waveplates combined with the polarization-dependent reflection loss from the Brewster surfaces of the plates. The plates are mounted together in the laser cavity so that they can be rotated about the normal to the plates, thereby changing the angle of the crystal axis with respect to the laser polarization (parallel to the plane of incidence) while maintaining the Brewster-angle orientation of the quartz surface relative to the laser mode propagation direction. For a given plate thickness and orientation of the optic axis, the plate will act as a wavelength-dependent waveplate, which in general changes the polarization character of the input laser mode. At some wavelength the polarization of the light that exits each plate will be the same linear polarization (p -polarization) that entered and, thus, will pass with no loss through the subsequent Brewster surfaces. In general the polarization of the beam will be elliptical upon exiting each of the plates and will therefore experience reflection loss at the Brewster surfaces that it encounters in traversing the rest of the laser cavity. Birefringent plates with integrally related thicknesses can provide enough selectivity that lasing will be restricted to one color (a few cavity modes) within the dye gain curve. It is interesting to note the frequency selectivity of the birefringent filter, in the laser cavity, is higher than that of a traditional Lyot filter with polarizers. The net spectral width of a cw dye laser with only a three-plate birefringent filter can vary significantly depending on alignment; widths can vary from 1 to more than 100 GHz (Nieuwesteeg *et al.*, 1986). The loss provided by a single Brewster surface for a beam incident with a polarization that is orthogonal to Brewster's polarization is

$$\text{loss} = 1 - \left(\frac{2n}{n^2 + 1} \right)^2. \quad (5.6)$$

Here n represents the index of refraction of the Brewster plate, and the loss is the fractional reduction in power of the transmitted beam. A net gain reduction of less than 1% is usually sufficient to suppress other modes from lasing. A typical birefringent filter will have a free spectral range of ≈ 100 nm. A dye laser with a three-plate birefringent filter has at least eight Brewster surfaces (including the jet surfaces) that can provide a net loss of $\approx 4\%$ for a 200-GHz detuning (this corresponds to the FSR of the thin etalon, see Fig. 5.9).

Usually etalons provide the next two higher levels of frequency selectivity. These parallel plate interferometers have the standard Fabry-Perot transmittance (Born and Wolf, 1964),

$$I(\delta) = \frac{I_0}{1 + F \sin^2\left(\frac{\delta}{2}\right)} \quad (5.7)$$

where $F = \frac{4R}{(1-R)^2}$ and $\delta = \frac{4\pi nL}{\lambda} \cos \theta$.

Here R represents the power reflectance of the etalon's surfaces (assumed equal), n its index of refraction, L its thickness, and θ the angle between the etalon normal and the optical propagation direction inside the etalon. λ is the vacuum wavelength. A useful measure of the etalon's resolving power is its finesse, \mathcal{F} , which is given by,

$$\mathcal{F} = \pi \frac{\sqrt{F}}{2}. \quad (5.8)$$

A cw ring dye laser might have one thin etalon ($L = 200 \mu\text{m}$ with $R = 30\%$) and one thick etalon ($L = 1 \text{ cm}$ and $R = 30\%$), which, when combined with the birefringent filter, provide sufficient frequency-selectivity to force the laser to oscillate on a single longitudinal mode.

The frequency-selective components that we consider here are typical of single-frequency dye lasers used in 1989, but other frequency-control systems have also been developed. As noted earlier, the high gain of the dye laser allows some experimental flexibility in testing ideas about laser design. The system with a birefringent filter and two etalons is the most popular because of its dependability and relative ease of construction. That is not to imply that this system is optimum. The tuning elements that are alternatives to the birefringent filter are prisms and the tuning wedge that is now rarely used. A variety of interferometric methods have also been used to control the frequency of dye lasers. These include the Michelson, Fox-Smith, and Mach-Zehnder interferometers and multiple implementations of these. Interferometers generally compete for the higher selectivity roles normally filled by the etalons.

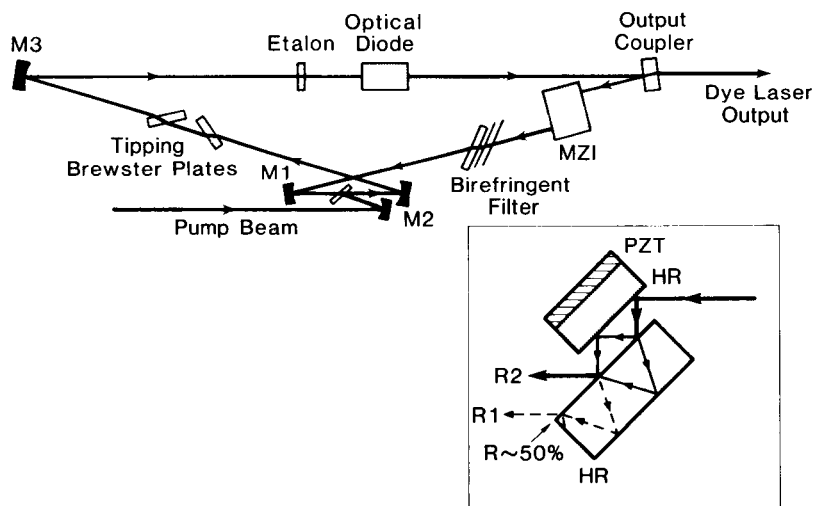


Fig. 5.10 Diagram of a single-frequency ring dye laser that uses a Mach-Zehnder interferometer for longitudinal mode control. This laser also uses a birefringent filter and a thin etalon for frequency selectivity. An optical diode is used for unidirectional operation and tipping Brewster plates are used for frequency scanning. The inset shows the structure of one type of intracavity Mach-Zehnder. This interferometer is constructed from two high-quality optical flats. One piece has a 50% reflectivity coating on its front surface and a high reflectivity coating (HR) on the back surface. The partial reflecting surface splits the input beam into two paths through the interferometer. The other optical flat is a high-reflectivity mirror and is mounted on a PZT translator so that the passband of the interferometer can be changed. The Mach-Zehnder has two output ports (R1 and R2). If the reflectivity of the partial reflector is 50%, and the losses in the two paths through the interferometer are matched, the contrast in the output ports can be 100%. With good low-loss coatings, the net insertion loss of this device in the laser cavity can be very small. Figure reprinted with permission from Bergquist and Burkins (1984).

One of the most intriguing of the interferometric frequency selectors for use with dye lasers is the Mach-Zehnder system that was proposed and developed by Bergquist and Burkins (1984). An example of one of the several possible implementations is diagrammed in Fig. 5.10. The advantage of the Mach-Zehnder interferometer is that, in principle, it can provide the necessary frequency-selectivity with substantially less excess loss than that of a comparable etalon. The reason for the unavoidable loss with intracavity etalons is that it is necessary to tilt the etalons away from normal incidence to avoid the disruptive effects of optical feedback on the oscillating mode of the laser. Tilting the etalon eliminates the feedback but we pay the penalty that power is lost from the laser mode. In laser jargon, this “etalon walkoff loss” results from the multiple reflections within the tilted etalon that bounce laser power out of the spatial mode of the laser

cavity. A properly balanced Mach-Zehnder system does not have this limitation because the only additional optical output port (beam R1 in Fig. 5.10) has zero output under proper operating conditions. This occurs when the Mach-Zehnder interferometer is set for a interference maximum on beam R2 (which corresponds to a minimum for beam R1) and when the interference maximum is tuned to a longitudinal mode of the laser cavity. In this case the only excess loss introduced by the Mach-Zehnder to the laser is that due to the absorption and scattering from the optical coatings, which can be made negligibly small. In practice the Mach-Zehnder system has seen only limited application but appears to have great potential.

The most important attribute of dye lasers is their tunability. In addition to reaching a particular wavelength, we frequently want to scan the frequency of the laser over some region near this wavelength. Depending on the spectral resolution that is required, it may not be necessary for the laser to oscillate on a single longitudinal mode. For example, the spectral features observed in solid-state spectroscopy are relatively broad, which often means that the resolution provided by multimode dye lasers is adequate. In this case a dye laser with only a birefringent filter provides enough resolution, and the laser can be scanned simply by tuning the bandpass of the birefringent filter. On the other hand, the technology required to tune and continuously scan the frequency of single-mode (single-frequency) dye lasers is complicated by the many frequency-selective elements. It is necessary to individually center and then scan all of these elements synchronously. Such scanning systems have been developed and some even actively optimize the centering of the bandpasses of the frequency-selective elements. The actively controlled systems provide long-term mode stability and repeatable scans. More sophisticated dye-laser control systems incorporate computer-controlled wavelength calibration, frequency scanning, and data acquisition (Marshall *et al.*, 1980; Williams *et al.*, 1983; Clark *et al.*, 1986).

For a deeper understanding of the methods of laser-frequency control we focus attention on a typical tuning system for a single-mode ring dye laser (such as in Fig. 5.6). We assume that the frequency-selective elements are able to force the dye laser to operate on a single longitudinal mode of the laser cavity. The optical length of the cavity then determines the fine tuning of the laser frequency. The laser frequency can be adjusted over a small range by using the piezoelectrically translated mirror, PZT (see Fig. 5.6), and larger-frequency changes are induced by rotation of the Brewster plate. Changing the optical length of the cavity will scan the laser but only within the bandpass of the thick etalon. Since the thick etalon has enough resolution to select a single mode it also limits the scan to less than the laser cavity FSR. In order to achieve longer scans, the thick etalon

must be scanned synchronously and likewise eventually the thin etalon must also be scanned. Usually these etalons are scanned with a piezoelectric translator to change the spacing between the plates of the thick etalon and by using a galvo-motor to rotate the thin etalon.

The alignment of the thick-etalon transmission peak to the cavity mode is critical and usually requires an automatic electronic servo to keep its bandpass properly aligned with the laser-cavity mode. This can be accomplished by using a conventional "modulation lock" which will be discussed shortly. For long scans it is necessary to tilt the thin etalon to track the thick etalon, but because of its low resolving power it is usually not necessary to have automatic feedback control—although such systems have been developed (Biraben and Labastie 1982). Tracking of the thin-etalon bandpass to a scanning laser frequency is also complicated by the fact that the bandpass of a tilted etalon scans approximately quadratically as a function of the tilt angle (see Eq. 5.2). This nonlinearity can be electronically compensated by using an electronic square-root-function module. Centering the passband of the birefringent filter is usually done manually by finding the maximum laser output power on a given mode. Automatic control systems for the birefringent filter can also be made by monitoring the polarization of the laser's output, which becomes slightly elliptical when the birefringent filter's bandpass is not properly centered on the cavity mode (Biraben, 1989).

A typical dye-laser scanning system thus consists of a Brewster plate rotated by a galvo-motor, a piezoelectrically driven thick etalon to track the specific cavity mode, and a thin etalon that is tilted by a galvo-motor to track the thick-etalon scan. All of these scanned elements are synchronized by a master control circuit that thus controls the laser's frequency. Commercial single-mode dye-laser systems can be scanned continuously with direct electromechanical control over ranges of about 30 GHz. Longer scans are certainly possible but they would put more stringent requirements on the electromechanical stability of the tuning elements. For example, with 1-MHz resolution, a 30-GHz scan already provides 3×10^4 resolution elements, which is usually adequate for most applications. There are some limits to the mechanical and electrical stability, linearity, and reproducibility of the electromechanical transducers used to position the tuning elements. Instability in these systems translates directly to laser-frequency fluctuations. In practice it is difficult to achieve 10 parts per million resolution in the electromechanical positioning. One can reconstruct a broader spectrum by computer-driven piecewise scans of about 30 GHz each. The total scan is then limited only by the bandwidth of the dye, but care must be taken to maintain some frequency reference in putting all of the separate scans together.

Pressure scanning of dye lasers is an alternative approach to mechanical scanning. As of the late 1980s, pressure scanning is not very popular, but it has some advantages. For example, it does not require moving parts in the laser. The idea is to enclose the entire laser inside a pressure-tight vessel so that when the pressure is changed the optical path length changes (due to changes in the index of refraction of the gas) and this causes the laser's frequency to change. If the etalons are designed with an open air space between the etalon surfaces, then when the pressure is changed, the etalons scan synchronously with the laser frequency.

4.2. Frequency-Stabilization Methods

The nature of the frequency fluctuations of lasers (as with other oscillators) is such that the measured frequency-stability depends on the time scale over which the measurement is made. The spectrum of dye laser frequency fluctuations is strongly peaked at low Fourier frequencies and then tapers down to a white noise level at high frequencies. In addition strong resonant peaks in the spectrum of the frequency noise result from a variety of technical problems (for example, noise at the AC line frequency). It is common practice to specify a laser's frequency-stability by a short-term "linewidth" and a longer-term center-frequency stability or drift rate. The implicit assumption here is that short-term fluctuations of the laser's phase determine the "linewidth," while slower fluctuations and drift dominate the stability the laser's center frequency. This model of the lasers frequency fluctuations has enough validity to be useful but it is far from the complete picture.

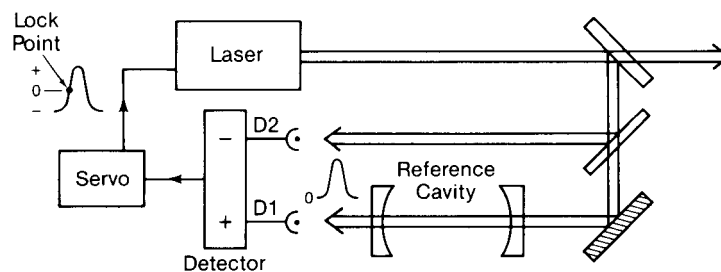
The frequency of the single-mode dye laser is determined by the boundary conditions imposed by the optical length of its resonator, which are usually arbitrary and generally lack long-term stability. The solution to the problem of frequency instability and inevitable drift is to lock the laser to a frequency reference such as a stable reference cavity or a molecular resonance. In principle the ultimate stability of the laser frequency can match that of the reference cavity if the control system is properly designed. Usually systematic errors degrade this performance considerably. Standard stabilized dye-laser systems have linewidths of ≈ 1 MHz with a center frequency of $\approx 5 \times 10^{14}$ Hz. Typical drift rates are about 10 kHz/sec, which is adequate for most experiments. The best cavity-stabilized laser systems have laser-frequency drift rates of about 1 Hz/s (Salomon *et al.*, 1988; Hils and Hall, 1989; Helmcke *et al.*, 1987). This outstanding performance exceeds the precision that is required for all but the most demanding metrology and physics experiments.

The other compelling reason to have a stable reference cavity is that it

can act as a fast frequency discriminator with a very large signal-to-noise ratio. The error signal derived from the cavity is then used in an electronic servo system to narrow the laser's linewidth and hence improve its resolution. The resulting linewidth of a laser stabilized to a reference cavity will depend on the laser's intrinsic frequency-fluctuation spectrum, the reference cavity's resolution, the servo system's bandwidth, and even the observation time. Some knowledge of the methodology of frequency-control systems is useful in developing an understanding of the operational characteristics of high-resolution dye lasers (see also Balykin *et al.* (1987) and Helmcke *et al.* (1982, 1987). Some of the common frequency-stabilization techniques are outlined in the following section.

4.2.1. Cavity-Side-Lock

One of the easiest and most generally applicable frequency-control methods is the cavity-side-lock system. It has been with us at least since the early days of the dye laser. This system uses a spectrally sharp Fabry-Perot transmittance peak to derive an electronic error signal that can be used to lock the laser to the side of the cavity resonance (see Fig. 5.11). The error signal is the difference between the photocurrents of the cavity transmittance peak (signal channel detected by D1) and the laser power (reference channel detected by D2). The light levels are adjusted so that the output from the difference amplifier is 0 when the laser frequency is tuned to the side of the cavity resonance. This provides a smoothly varying monotonic frequency discriminator for laser frequency excursions less than $1/2$ of the



Cavity Side Lock

Fig. 5.11 Laser frequency control by the cavity side lock method. Part of the laser's output beam is directed into a Fabry-Perot cavity and onto a photodetector D1. A reference beam is directed onto detector D2 which measures the laser's power. The transmission function of the Fabry-Perot cavity is shown schematically near D1. The cavity acts as a frequency discriminator for the laser. The error signal is generated from the difference between the signals from D1 and D2, and is shown with the lock point indicated at zero voltage. A servo amplifier uses the error signal to control the laser's frequency.

cavity-resonance width. Depending on the overall sign of the correction signal, the laser frequency can be locked to one side of the fringe or the other. The zero crossing of the error signal is set at the point of fringe half maximum by adjusting a variable attenuator in the reference channel. The DC offset of the reference channel is derived from the laser power rather than from a voltage reference for a good reason. This reference signal generated by the laser power cancels laser-amplitude fluctuations that would otherwise cause an error in the lock signal. This is an important correction because, as we shall see, the amplitude fluctuations on dye lasers are often relatively large. Details of an advanced side-lock frequency-control systems can be found in Helmcke *et al.* (1982).

4.2.2. Modulation Lock

A second and very useful method of laser-frequency stabilization is the modulation lock. This system incorporates frequency modulation and synchronous detection to generate an error signal that is then used to lock the laser to the peak of a resonance. The resonance can be a Fabry-Perot cavity transmission signal but it can equally well be an atomic or molecular resonance. This method is very general and it allows us to stabilize any variable parameter to the maximum or a minimum of a response function. Because of the simplicity of the method and because we often want to maximize (or minimize) some response, the technique is widely used in servo-control systems. We described this method in terms of locking the oscillation frequency of a laser to the peak of a Fabry-Perot transmission fringe. The important features of the modulation lock are illustrated in Fig. 5.12a, 5.12b. The various electronic signals are shown in Fig. 5.12b where the Fabry-Perot transmission fringe is displayed as a function of the laser frequency. If the laser frequency is sinusoidally modulated about the peak of the cavity resonance, the transmitted light intensity varies as the second harmonic of the modulation frequency. However if it is modulated about the side of the cavity resonance, the transmitted power will vary at the modulation frequency with a phase that depends on which side of the fringe the laser is tuned. There is a 180° relative phase shift of the modulation response on the two sides of the fringe. The power of the laser light transmitted through the cavity is then detected and demodulated using a lock-in amplifier. The lock-in output is then lowpass filtered to produce the discriminator-shaped output (see Fig. 5.12b). This discriminator signal is used as the error signal for the servo-control loop. The phase reversal of the error signal across the fringe changes the sign of the output from the lock-in and produces an error signal that crosses 0 at the peak of the resonance. For small-modulation amplitudes, the shape of the discriminator signal is approximately the first derivative (with respect to frequency)

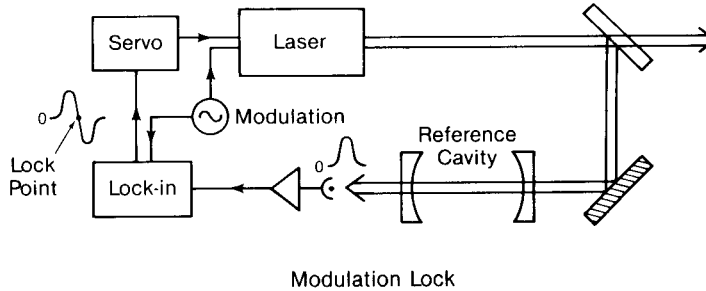


Fig. 5.12a Laser frequency control by the modulation lock method. A Fabry-Perot reference cavity is used as a frequency discriminator for the laser. The cavity's transmission function is indicated schematically near the photodetector and amplifier. The signal from the detector goes to the lock-in amplifier where it is compared with the modulation signal that is used to modulate the frequency of the laser. The lock point is indicated on the error signal that is shown schematically as the output of the lock-in. A servo amplifier uses the error signal to control the laser's frequency.

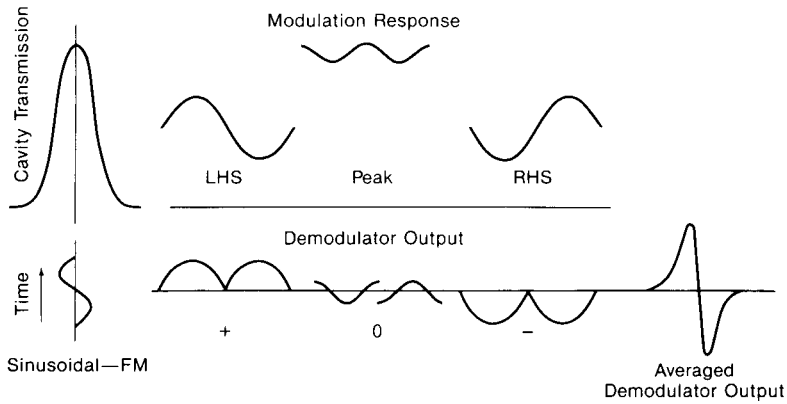


Fig. 5.12b Signals used in the modulation locking method. The cavity transmission function and the modulation of the laser's center frequency are displayed on the left-hand edge of the figure. The center of the figure shows the variation of the cavity's transmission due to the modulation and is displayed as a function of the laser's center frequency relative to the cavity resonance. The demodulator (lock-in) inverts the modulation response synchronously every half-cycle of the modulation. Its output is shown at the bottom of the figure. When the demodulator's output is averaged for times that are long compared with the modulation frequency, the result is an output signal that is approximately the derivative of the cavity transmission function. This output is shown at the bottom right of the figure and is displayed as a function of the laser's center frequency.

of the transmission function. Similarly, high-order approximate derivative signals are obtained by demodulating the transmitted power at harmonics of the modulation frequency. For example, a third derivative locking signal is obtained by demodulating at the third harmonic of the modulation frequency and it has some advantages with respect to systematic errors. These frequency modulation–demodulation ideas are also useful for reducing noise and background problems in spectroscopy (e.g., laser derivative or FM spectroscopy).

4.2.3. *rf-Optical Heterodyne Lock*

Another laser stabilization system has been developed using rf heterodyne techniques (Drever *et al.*, 1983; Hough *et al.*, 1984; Helmcke *et al.*, 1987). Of all of the methods, this “rf-optical heterodyne” locking system has demonstrated the best performance, in terms of both center frequency control and the narrowest linewidths. The method is similar to the modulation lock described previously, with the distinction that it uses radio- or microwave phase modulation on the laser’s output to generate laser sidebands that lie outside the resolution width of the resonance of interest. The high modulation frequencies are advantageous in suppressing noise, in achieving high-servo-control bandwidths, and in achieving good transient response characteristics. An example of an optical heterodyne system used for laser-frequency stabilization is diagrammed in Fig. 5.13. Here the system consists of a laser, an electro-optic phase modulator (ϕ mod, made from a crystal of ADP, ammonium dihydrogen phosphate), an optical directional coupler (made from two polarizers and a Faraday rotator), a precision reference cavity, a photodetector (det), some filters, a balanced mixer, and a servo-control amplifier. The cavity resonance is detected in reflection by this heterodyne technique and can provide two types of signals. These signals are derived from the two detection quadratures of the balanced mixer (determined by the phase of the reference signal) and correspond to the cavity transmission and dispersion functions. The cavity resonance acts to alter the pure phase modulation that was imposed on the laser light by the electro-optic modulator. This alteration of the phase modulation comes from the transmittance and phase shift of the laser light by the cavity. The cavity thus converts some of the phase modulation into amplitude modulation, which is then detected by the photodetector and subsequently demodulated by the mixer to generate a baseband (DC) response. The phase of the reference signal (derived from the original modulation signal) that is applied to the mixer determines the detection quadrature and, thus, whether we detect the effect of cavity transmittance or dispersion. Typical response signals for the two detection quadratures are shown in Fig. 5.14. The discriminator shape of the dispersion signal provides an excellent error

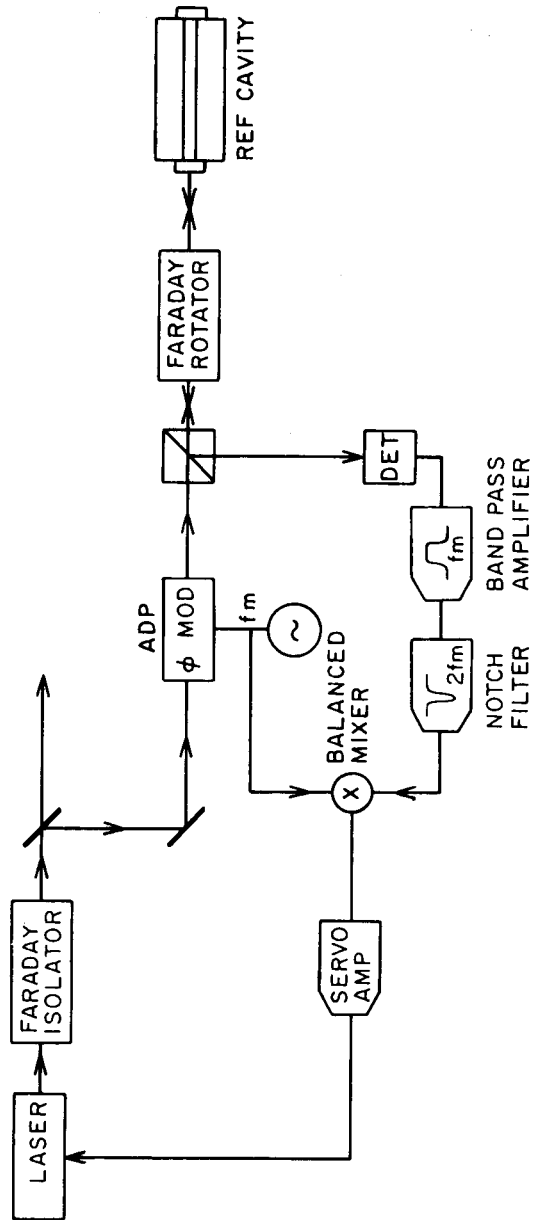


Fig. 5.13 Laser-frequency stabilization system using rf-optical heterodyne locking method. Part of the laser's output is phase-modulated using an electro-optic modulator (ϕ -mod). The phase-modulated laser beam then probes the reference cavity and is detected in reflection by the photodetector DET. The resulting signal at the modulation frequency passes through a set of filters to the balanced mixer. There it is mixed with a reference signal at the modulation frequency to produce the error signal (see Fig. 5.14) that is used by the servo-amp to control the laser's frequency. This figure is reproduced with permission from Drever *et al.*, (1983).

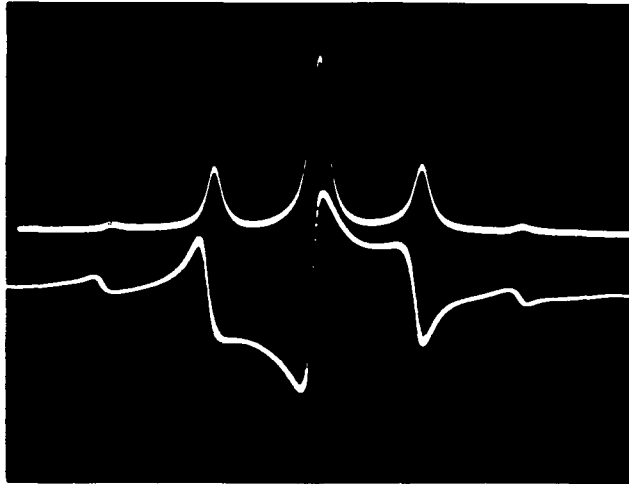


Fig. 5.14 Cavity signals generated by the rf-optical heterodyne locking method. The output of the mixer (from Fig. 5.13) is shown as a function of the laser's frequency which is scanned. The upper trace shows the output when the phase of the reference signal (applied to the mixer) is set to detect the cavity's transmission. The multiple-peaked structure results from the carrier and sidebands being transmitted into the cavity when they come into resonance. The carrier (large peak in the center) and the two adjacent sidebands are separated by the modulation frequency. Small peaks due to the second-order sidebands are also visible at a spacing that is twice the modulation frequency. The lower trace shows the output when the phase of the reference signal is shifted by $\pi/2$. It represents the effect of cavity dispersion as seen by the phase-modulated laser beam. The dispersion signal has a steep discriminator shape that crosses 0 when the carrier is tuned to the peak of the cavity resonance. This discriminator is used as the error signal in the frequency-control loop. This figure is reprinted with permission from Drever *et al.* (1983).

signal for laser-frequency control. Some of the components in this system can be compared directly to those of the modulation lock; the phase modulator serves the role of the laser FM, and the mixer replaces the lock-in amplifier. One important advantage of the heterodyne system is that the high modulation frequencies and the detection of the cavity in reflection allow the time scales of the detection process to be very short. This allows the response time of a servo system to be shorter than the characteristic response time of the cavity (Drever *et al.*, 1983) while maintaining a good signal-to-noise ratio. This is an important consideration for the high-speed servo systems that are required for very narrow laser linewidths. This method has been used by Bergquist and collaborators to observe ≈ 50 -Hz-wide mercury-ion resonances; this indicates that the dye laser's linewidth and center frequency stability are at least that good (Wineland *et al.*, 1989).

4.2.4. Polarization Lock

Noteworthy because of its good performance and simplicity is a related laser-frequency-stabilization method that was developed by Hänsch and Couillaud (1980). Analysis of the polarization state of the light reflected from the cavity is used to detect the dispersive nature of the cavity resonance. This method has the advantages that it produces a discriminator-shaped signal without modulation and it has a very large capture range. This results in a robust laser-locking method that is useful for laser-frequency stabilization and optical buildup cavities.

4.2.5. Postlaser Stabilization

An exciting and relatively new development in laser-frequency control is the implementation of a postlaser-frequency-correction system (Hall and Hänsch, 1984; Hall *et al.* 1988). The concept is that with the appropriate acousto-optic and electro-optic transducers, we can correct the frequency errors on the laser beam after the beam exits the laser. A system of this type is diagrammed in Fig. 5.15. The external frequency correction is implemented with an acousto-optic frequency shifter (driven by a voltage-controlled oscillator) and an electro-optic modulator (EOM). The EOM acts as frequency transducer through its ability to induce a time-dependent optical phase shift via its electric-field-dependent index of refraction. In this case the change in the laser frequency is proportional to the derivative with respect to time of the applied electric field. Thus the circuitry for the electronic feedback to the EOM is complicated by the fact that adding a fixed frequency shift to the laser requires that a voltage ramp be applied to the EOM. The EOM used in this way operates as an optical phase shifter and hence only works well for removing high-frequency fluctuations. The acousto-optic transducer is required for the low frequency fluctuations and fixed frequency offsets. Another challenge is the fact that the time scales for the response of the acousto-optic and electro-optic transducers are very different and appropriate crossover compensation must be designed. Clever solutions to these challenges have been developed by Hall and Hänsch (1984). The error signal for this system can be derived from any of the methods described previously, but perhaps the most appropriate is the rf-optical heterodyne method. Impressive performance has been achieved with these postlaser stabilization systems but, unfortunately, they are not available commercially as of 1989. Starting with a single-mode dye laser that had an intrinsic linewidth of ≈ 1 MHz, the postlaser stabilization methods have produced linewidths on the order of 1 kHz. Even better performance can be anticipated. Another application of this method has been to make an optical phase lock between a cw dye laser and a HeNe laser

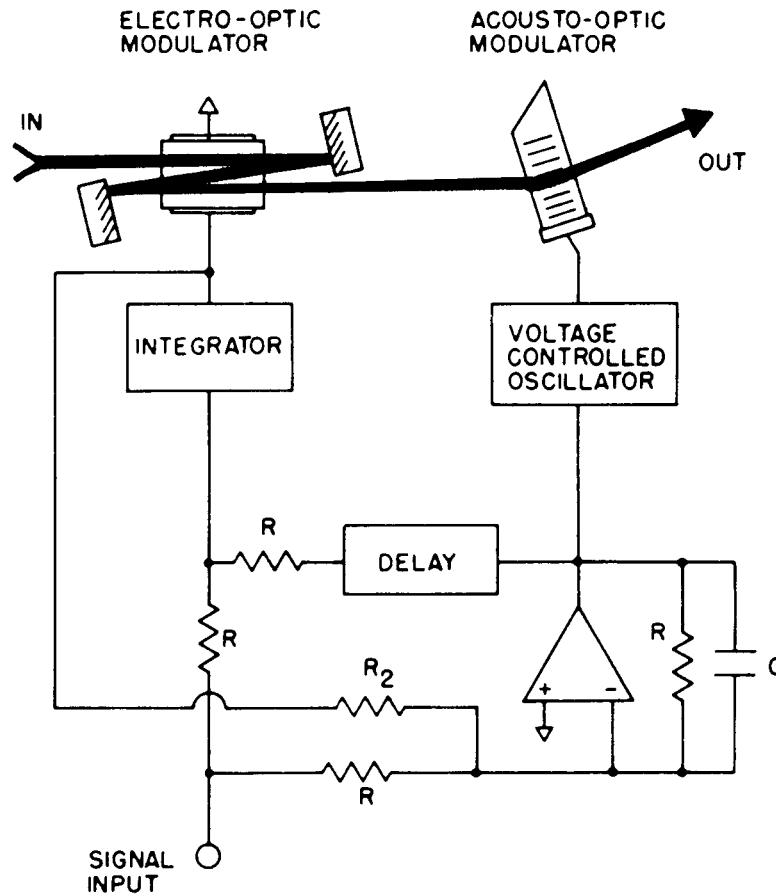


Fig. 5.15 Laser-frequency control by the post-laser-stabilization method. In this system the frequency of the laser's output is changed outside the laser by an electro-optic modulator and an acousto-optic modulator. A time rate of change of voltage applied to the electro-optic crystal will change the frequency of the laser beam by a small amount. Larger frequency shifts are generated by the acousto-optic modulator which is driven by a voltage-controlled oscillator. To optimally use the two transducers the input error signal is first processed electronically as indicated. Figure reprinted with permission from Hall and Hänsch (1984).

that was used as the reference oscillator (Hils and Hall, 1989; Salomon *et al.*, 1988).

It is humbling for laser scientists to learn that many of the basic principles in these methods had been developed in the pre-laser days by scientists working with rf and microwave systems. The techniques were subsequently "reinvented" with laser technology.

Up to this point I have outlined various general techniques for deriving an error signal from a resonance, but have not discussed the requirements for a feedback loop that can use this error signal to control the laser frequency. The loop needs to process the error signal and drive the appropriate transducers to correct the laser's frequency fluctuations. The loop will thereby null (or attempt to null) the error signal. Common dye laser frequency transducers are galvo-motor-driven Brewster plates, piezoelectrically mounted mirrors, and electro-optic crystals (see Fig. 5.6). Each of these transducers can change the optical path length of the laser cavity and hence the laser frequency. Typical commercial frequency-stabilized dye-laser systems use a galvo-driven Brewster plate and a piezo-mounted mirror for their frequency-control transducers. These systems routinely achieve laser linewidths on the order of one MHz. With faster feedback control and better reference cavities it is possible to achieve laser linewidths of about 20–100 kHz with a piezo-mounted mirror and a galvo-driven Brewster plate. For very high resolution applications an electro-optic modulator (EOM) can be included in the laser cavity. With the EOM, dye-laser linewidths on the order of 50 hertz have been demonstrated and linewidths of one hertz or less are anticipated. These are truly impressive high-resolution oscillators when we recall that the oscillation frequency is $\approx 5 \times 10^{14}$ Hz. The narrow linewidths achieved with the intracavity EOMs are due to the high-speed response of the crystal and the high servo bandwidths that are possible. In general the higher the servo bandwidth, the narrower the resulting laser linewidth. The actual performance of the frequency-stabilization system depends on the spectral density of the frequency noise on the laser and the characteristics of the servo loop. In principle, and in some cases in practice, laser linewidths as narrow as you desire can be achieved with late 1980s technology (Hils and Hall, 1989). Often the limitation to the resolution is not the laser at all but rather the spectroscopic sample of interest.

Optimization of the filter characteristics of the feedback loop can be a difficult task given the complexity of the system with the multiplicity of transducers. In addition we need to take into account the spectrum of the dye laser's frequency noise and the laser's dynamics. The simplest control loops (termed proportional locks) use purely proportional control, where the feedback is linearly related (by the gain) to the error signal. These control systems are very stable but are lacking in both accuracy and dynamic response. A significant improvement in performance is obtained by integrating the error signal with respect to time before feeding back to the transducers. An integrating loop filter has gain that rolls off toward higher frequencies at a rate of 6 dB per octave for each stage of integration. Even a single-stage integrating-loop filter has the advantage that is

guarantees zero error at DC and only a fixed, finite error for a ramping error signal. In contrast, the proportional control loop will in general always have a finite error. Adding some derivative feedback in the loop can often improve the dynamic response. It is common practice to use some combination of proportional, integral, and derivative feedback. These systems are best optimized with careful system analysis, but empirical adjustment of the gains and time constants is often productive.

As we have discussed, most of these laser-locking methods can be applied equally well to stabilizing the frequency of lasers to a cavity or to atomic or molecular resonances. In the latter case the most applicable techniques are the modulation lock and the rf heterodyne lock. The ability to stabilize the laser to an atomic resonance is important for some spectroscopic applications and is crucial for high-accuracy metrology and laser-frequency standards. The atomic and molecular resonances cannot provide the same signal-to-noise ratio that is available from a cavity, but their long-term (say, for times longer than a few seconds) stability is generally much better. For dye lasers to have high resolution and high accuracy, it is customary to lock the laser's frequency to a high-Q reference cavity (to achieve the narrow linewidths) and then to lock the cavity to an atomic or molecular resonance (which then provides the long-term stability).

The transformation of a broadband dye laser into a frequency-stabilized narrow-linewidth laser adds considerably to the cost and complexity of the laser system. There is also a penalty to be paid in the available output power when we add intracavity optical elements (this typically amounts to about a factor of 2). If we use an electro-optic crystal, the upper power limit may also be reduced due to the limited optical-power density that the crystals can endure.

In summary, commercial stabilized dye-laser systems can provide high resolution (≈ 1 MHz) with tunability and good power levels. Their tuning range extends throughout the visible and near-visible part of the spectrum. These high-resolution systems are more than adequate for most spectroscopic applications. For applications that demand higher resolution, very narrow-linewidth dye-laser systems have been developed in a number of research laboratories. The systems with the best reported resolution generally use optical heterodyne techniques and EOMs to achieve laser linewidths below 100 Hz. I see no reason that the linewidths could not be reduced further to below one Hz in the future. So while the performance levels achieved in 1989 are truly impressive, they are merely a glimpse of the present state of the art and they will certainly be surpassed.

5. SPECTRAL CHARACTERISTICS

The complexity of dye lasers encourages the user to have some diagnostic instruments to monitor the laser's output characteristics. Useful diagnostic tools include power meters as well as wavelength- and linewidth-measuring devices.

With dye tuning ranges of about 100 nm and linewidths of about 10^{-6} nm it is not a trivial task to determine, with precision, the lasing wavelength of cw dye lasers. Many interferometric instruments have been developed to measure the laser's wavelength relative to known standards; these include the lambda or wave meter, the sigma meter, the Fizeau wavemeter, calibrated Fabry-Perot interferometers, and dispersive birefringent filters (Juncar and Pinard, 1975; Kowalski *et al.*, 1976, 1978; Hall and Lee, 1976a; Woods *et al.*, 1978; Snyder, 1980; Williams *et al.*, 1983; Lichten 1985, 1986; DeVoe *et al.*, 1988). The accuracy of these interferometers varies from 5 to 8 digits. Special standards-laboratory instruments are capable of 10 digits of accuracy in wavelength measurement. Also extremely useful for general laboratory spectroscopy are the wavelength tabulations that exist for molecular spectra of some simple molecules, such as those for I_2 (in the red) (Gerstenkorn and Luc, 1978) and Te_2 (in the blue) (Cariou and Luc, 1980). These tabulations can be used to determine a dye laser's wavelength to about 3×10^{-7} .

We need certain mathematical and experimental tools to characterize the spectral properties of lasers. These tools certainly include the frequency and amplitude-noise spectral densities and maybe the Allan variance. The Allan variance was developed to quantify the frequency stability of oscillators and can be applied directly to lasers. It is discussed here because of its usefulness and its popularity in the literature and also because it is not found in the usual textbooks.

5.1. Amplitude Fluctuations

The spectral distribution of amplitude noise in the output of a single-frequency dye laser contains a great deal of useful information. It can be measured directly by monitoring the laser light with a fast photodetector and a rf-spectrum analyzer. The quantum theory of the laser predicts that the fluctuations in the power from an ideal laser source will be determined by the statistics of the quantum mechanical generation of the photons (Sargent *et al.*, 1974; London, 1983). In this model the ideal laser would produce light with a time distribution of photons that is Poissonian. Upon

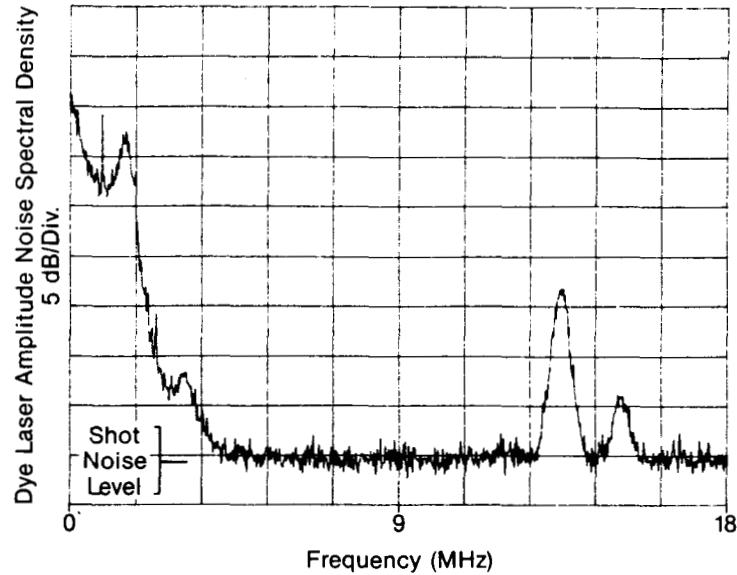


Fig. 5.16a Spectral density of the amplitude noise of a single-mode ring dye laser. The noise on the laser's output power is strongly peaked at the lower frequencies and finally reaches the shot-noise level at a frequency of about 4.5 MHz. The broad peaks in the noise come from small amounts of power oscillating in transverse modes in the argon pump laser. These pump-laser-related noise peaks extend out to hundreds of megahertz but spectral regions can be found where the dye laser's amplitude noise is shot-noise-limited.

detection this photon distribution generates a Poissonian photoelectron distribution and hence produces the usual "shot-noise" fluctuations in the photocurrent,

$$i_{\text{SN}} = (2eiBW)^{1/2}. \quad (5.9)$$

Here i is the detected photocurrent, e is the electron charge, and BW is the detection bandwidth. The shot-noise distribution is spectrally flat. Figure 5.16a shows the measured spectral density of the amplitude noise of a good single-mode dye laser. The figure also indicates the expected shot-noise level for the same average optical power on the detector. Clearly, there is more going on in real lasers than is predicted by the quantum mechanical model of the ideal laser. Characteristically, the amplitude noise is very large at low Fourier frequencies and decreases progressively to higher frequencies until it reaches the shot-noise level at a frequency of approximately 4.5 MHz. We also see that there are many large resonant noise peaks throughout the spectrum. These are due to various technical noise

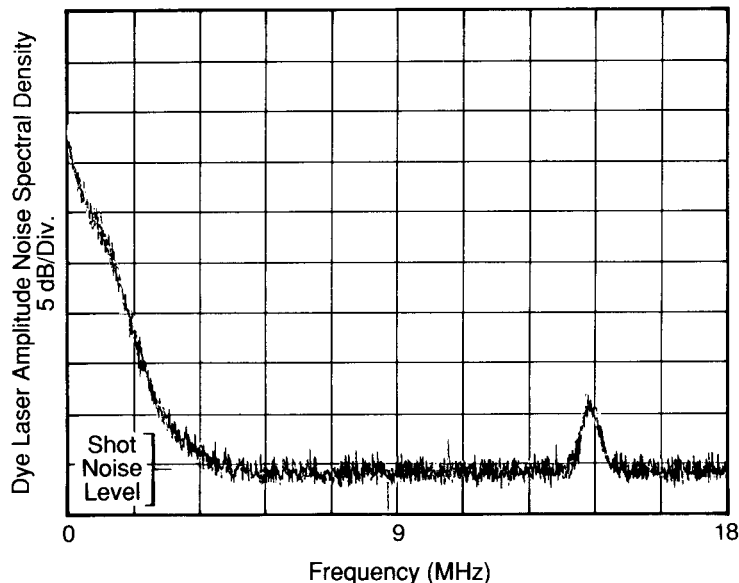


Fig. 5.16b Spectral density of the amplitude noise of the same dye laser as shown in Fig. 5.16a, but now with the aperture in the argon laser carefully adjusted to eliminate transverse modes. The dye laser's amplitude noise is improved, but the noise is still strongly peaked at low frequencies.

sources, the most important of which are the argon laser's intermode beats that are transferred through the gain of the dye jet to the dye laser's power (these intermode beats are observed out to several hundreds of megahertz). In Fig. 5.16b the spectral density of the amplitude noise of the same dye laser is shown but now with the argon laser resonator apertured to eliminate transverse modes. This removes most of the resonant peaks in the noise (in this frequency range) and significantly improves the dye laser's amplitude noise spectrum.

One of the important things we learn from the spectrum of amplitude noise is that any measurements that are made with a detection bandwidth centered at low frequencies (or near one of the resonant noise peaks) will be contaminated by excess noise on the laser. As seen in Fig. 5.16 this excess noise is not negligible. In this example there is ≈ 35 dB of excess noise at a detection frequency near 100 kHz (resolution bandwidth was 3 kHz). The noise is even greater at lower frequencies. Not surprisingly the signal-to-noise ratio can be improved by moving the center of the detection bandwidth to higher frequencies by using high-frequency modulation methods. If we look to high enough frequencies it is possible to reach the

shot-noise level in some limited-detection bandwidth. In fact, it is even, possible to achieve noise levels below this shot-noise level by using non-linear optical methods to generate nonclassical forms of light such as squeezed states. This regime of sub-shot-noise limited detection is a hot topic in modern optics with two compilations of papers on this and related subjects ("Squeezed States," 1987).

5.2. Frequency Fluctuations

One method for determining the frequency stability and linewidth of a dye laser is to monitor the laser's output with a high-resolution Fabry-Perot cavity (optical spectrum analyzer). These instruments are available commercially. Using a scanning Fabry-Perot cavity to measure the spectral distribution of light from a multimode standing-wave dye laser (with only a birefringent filter as the tuning element) shows the optical power distributed in a large number of discrete longitudinal modes. The spectral width of this array of modes can vary from 1 to 100 GHz. In this multimode case the distribution of modes is often unstable.

If the dye laser is made to run on a single mode, a high-finesse cavity can be used to determine the laser's linewidth and the spectral distribution of the residual frequency fluctuations. Another method for measuring the frequency stability of a laser is to use a fast photodiode to observe the beat note between the unknown laser and a narrow-linewidth reference laser. There is also the "self-heterodyne" method, which uses a fiber delay-line to measure the laser's linewidth.

The frequency noise spectrum of a single-mode laser can be measured best by detecting the rf spectrum of the heterodyne beat note between two lasers: the unknown laser and a reference laser that has a narrower spectral width (Hough *et al.*, 1984). This heterodyne method is generally preferred for the very high resolution systems but it requires an additional very stable reference laser to act as the local oscillator. A limitation here is that the linewidth of the very best lasers must be determined by deconvolution of two equally good lasers or by other methods (cavities or special narrow spectral lines).

The Fabry-Perot cavity method of measuring a laser's frequency-noise spectrum relies on using the cavity's transmittance or reflectance function as a frequency discriminator. By tuning the laser's center frequency to the side of the cavity resonance and measuring transmitted power, the cavity then acts to convert frequency fluctuations directly into amplitude fluctuations at the detector. A cavity (or a molecular resonance) can be an excellent frequency discriminator but care must be taken to avoid systematic errors (for example, detection bandwidth limits, cavity response time,

and laser amplitude noise). The literature is full of “outstanding” results based on improper measurements. A good example of a very popular mistake is to lock a laser’s frequency to some cavity or atomic resonance (by the methods described previously) and then monitor the error signal within the servo-loop to provide a measure of the residual frequency noise. This appears reasonable at first glance, but usually the error signal is contaminated at some level by systematic errors (such as a ground loop). These systematic error signals are then corrected by the servo system as if they were laser-frequency fluctuations. This puts these artificial errors directly on the laser frequency. Any measurement of the error signal would indicate that the laser’s frequency fluctuations are small, because the servo loop is acting to cancel the error signal. This gives a misleading result when the measured error signal is then used to calculate the laser’s frequency fluctuations. However, it is true that monitoring the residual error signal is useful in providing information about how well the servo electronics are working. It does *not* answer the question of how well the error signal represents the laser’s frequency fluctuations. To make a definitive statement about the frequency fluctuations of a stabilized laser it is imperative to have a measure of the laser’s frequency that is independent of the stabilization system.

The self-heterodyne method of measuring a laser’s linewidth uses a time delay and a heterodyne detector to produce the autocorrelation of the laser’s frequency noise at a given time delay (Okoshi *et al.*, 1980). This method compares the oscillation frequency of a laser at an earlier time with its oscillation frequency now. Self-heterodyne systems are very easily implemented by sending some of the laser’s output through a long fiber (for the delay) and then combining this fiber-delayed output with the direct output on a fast photodetector to observe the beat note. In these systems one of the two beams is usually frequency shifted by an acousto-optic modulator (for example, by 80 MHz) to avoid technical noise at zero frequency difference upon detection. It is difficult to make accurate measurements with this method if the laser has a very narrow linewidth, and in general care must be used to avoid misleading results (Kikuchi and Okoshi, 1985).

A spectrum of frequency fluctuations can be used to provide an effective laser linewidth (Elliot *et al.*, 1982). In two limiting cases, which depend on the analytical character of the frequency noise, the linewidth can be calculated trivially. The important factor here is whether the Fourier frequency of the dominant frequency fluctuations is high or low, compared with the rms frequency fluctuations of the laser. That is, are the main frequency excursions caused by low frequencies with a high modulation index, or high frequencies with a low modulation index, where high and

low are measured relative to the laser's rms frequency fluctuations. For example, if we make the assumption that the frequency-noise spectrum is rectangular with a bandwidth B , we can calculate the linewidth in these two limiting cases. If the laser's rms frequency fluctuations are large compared to the bandwidth of the frequency fluctuations, the laser's lineshape is Gaussian and the linewidth is given by

$$\Delta_{\text{FHM}} = 2(2 \ln 2)^{1/2} \delta_{\text{rms}}. \quad (5.10)$$

Here δ_{rms}^2 is the rms frequency deviation. On the other hand, when the bandwidth of frequency fluctuations is larger than the laser's rms frequency fluctuations, the laser's lineshape will be Lorentzian and the linewidth will be given by

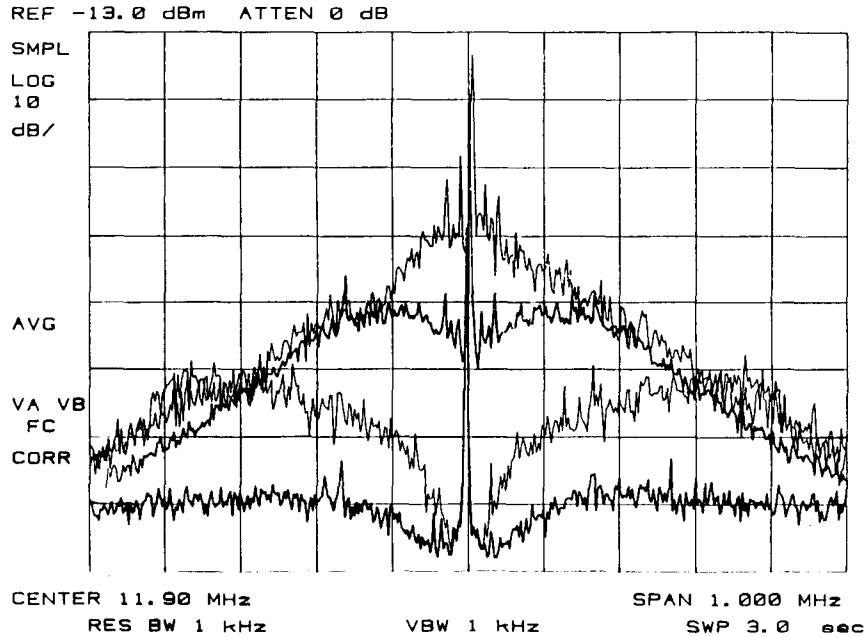
$$\Delta_{\text{FWHM}} = \pi \frac{(\delta_{\text{rms}})^2}{B}. \quad (5.11)$$

Here we have again simplified the problem by assuming that the spectrum of frequency fluctuations is rectangular in shape with a bandwidth B . In the more general case when the frequency fluctuations are not spectrally flat, with important contributions coming from both high and low Fourier frequencies, the lineshape and linewidth could be determined from the spectrum of frequency fluctuations by numerical integration of the equations given by Elliot *et al.* (1982).

As with the amplitude noise, the spectrum of frequency fluctuations for dye lasers is large at low frequencies and then falls off at higher frequencies. There are often numerous large resonances throughout the spectrum. Figure 5.17 shows the spectrum of frequency fluctuations of a single-mode ring dye laser that was measured with a high finesse cavity and a rf-optical heterodyne detection system. Also shown is the reduction in the frequency noise that is achieved when the frequency-control loop is turned on. In this case, the servo is able to reduce the frequency noise (as measured by the servo-loop error signal) by as much as 50 dB. An independent frequency discriminator would be required for an accurate determination of the laser's linewidth.

A mathematical tool that is genuinely useful in describing the frequency stability of lasers (and other oscillators) is the Allan variance (Allan, 1966; Allan *et al.*, 1974). It is the variance of the second difference of a series of consecutive frequency measurements. The Allan variance is defined

$$\sigma(\tau) = \frac{1}{\nu_0} \left(\frac{1}{2(M-1)} \sum_{i=1}^{M-1} (\nu_{i+1} - \nu_i)^2 \right)^{1/2} \quad (5.12)$$



Hall *et al* Summary for IQEC - 88 Tokyo, Japan July 18-22, 1988

Fig. 5.17 Spectral density of the frequency noise of a single-mode ring dye laser with and without fast frequency control. The frequency fluctuations are measured using the rf-optical heterodyne locking method (modulation frequency ≈ 12 MHz) diagrammed in Fig. 5.13. The vertical scale displays the dye laser's frequency noise with a sensitivity of 10 dB/div. The horizontal scale is 100 kHz/div and the data were taken with a resolution bandwidth of one kHz and a video bandwidth of one kHz. The largest peak shows the frequency noise on the laser without fast frequency control. When a fast postlaser frequency control loop (of the type diagrammed in Fig. 5.15) is implemented, the frequency fluctuations are reduced. The three lower curves show the effect of incrementing the control loop gain by about 10 dB per step. The frequency noise remaining in the lowest trace is near the noise level of the measurement system. It would correspond to a dye-laser linewidth of less than one Hz if the measurement of the error signal was an accurate measure of the laser's frequency fluctuations. Figure is reproduced with permission from Hall *et al.* (1988).

Here M is the number of successive frequency measurements (assuming no dead time between measurements), ν_0 is the mean laser oscillation frequency, and ν_i is the i th frequency measurement made during the sample interval time τ . The Allan variance can also be calculated from the power spectral density of the frequency noise $S(f)$ as follows:

$$\sigma^2(\tau) = 2 \int_0^{\infty} df \frac{S(f)}{\nu_0^2} \left(\frac{\sin^2 \pi f \tau}{\pi f \tau} \right)^2. \quad (5.13)$$

One of the wonderful properties of this function is that it is well behaved for common types of frequency noise, such as $1/f$ noise. This is not true for the usual standard deviation which is often divergent. The Allan variance serves as a one-parameter figure of merit for the frequency stability of oscillators. Without measuring the spectrum, it can provide a diagnostic of the type of frequency fluctuations that are present. For example, an Allan variance that decreases as $1/\tau$, where τ is the averaging time, indicates that the frequency noise spectral density is white.

6. SUMMARY

Cw dye lasers are a unique source of laser radiation with broad tunability, high spectral purity and good output-power levels. We have seen that these lasers can provide complete spectral coverage from 365 to 1000 nm with typical power levels that range from 0.1 to more than 1 W. Nonlinear optical techniques have been used to extend this spectral coverage into the UV (260–400 nm) by harmonic generation and sum frequency mixing and into the near-IR (2.2–5 microns) by difference frequency mixing. Other specific wavelengths not included here have been generated by nonlinear methods for special applications. Continued improvements in the pump lasers, the dyes, and the nonlinear optical materials will undoubtedly provide higher output powers and extended spectral coverage.

The spectral characteristics of cw dye lasers are both good and bad: good with respect to their linewidths and, hence, spectral-resolving capabilities, but generally poor with respect to their amplitude noise properties. The spectral density of amplitude noise on cw dye lasers is large for Fourier frequencies below a few megahertz. Because of necessity, techniques have been developed to alleviate the problems associated with this amplitude noise. Typical linewidths of cw frequency-stabilized dye lasers are ≈ 1 MHz, which is more than adequate for most applications. The technology is available to reduce the dye laser's linewidth to ≈ 1 Hz for those special applications that require it.

PROBLEMS

1. By making simple assumptions about the dye gain and available pump power, design a three-mirror folded linear dye laser cavity of the type shown in Fig. 5.2. For this cavity calculate the expected difference in frequency between the main longitudinal mode and the spatial hole-burning mode that could oscillate simultaneously.
2. Calculate the expected temperature rise of a laser dye (such as R6G in ethylene glycol) when it is pumped with 10 W of cw ion-laser radiation

- at 514 nm. Make reasonable assumptions about the optical and physical properties of the dye and the dye-circulation system.
3. Estimate the feasibility of pumping a cw dye laser with solar radiation. For this estimate propose some simple and realistic design for the laser.
 4. Assuming the spectrum of frequency noise shown in Fig. 5.17 is an accurate representation of the dye laser's frequency fluctuations, make an estimate of the contributions to the laser's linewidth due to the various spectral regions of the noise. To calibrate the vertical scale, use the fact that a perfectly coherent laser would produce a signal of -3 dBm (at 12 MHz) when the laser's center frequency was tuned to the half-power transmission point of the reference cavity. Note that the rf-heterodyne detection method transfers the frequency-fluctuation information from zero frequency to the modulation frequency (12 MHz in this case).
 5. Assume that the Fourier spectrum of a laser's frequency fluctuations is described by a simple power law dependence (that is, $S(f) = H_a \cdot f^{-a}$; $a = 2, 3/2, 1, 1/2, 0, -1/2,$ and $-1,$ and H_a is a constant).
 - (a) Find the functional dependence of the Allan variance on the averaging time τ .
 - (b) Determine which simple power laws also give a standard deviation (using the usual definition) that is well behaved.
 6. What sort of length stability is required for a Fabry-Perot reference cavity that is used to stabilize the frequency of a visible laser to one Hz? Can length stabilities with this performance be achieved given the physical properties of realistic materials?

REFERENCES

- Allan, D.W. (1966). Statistics of atomic frequency standards. *Proc. IEEE* **54**, 221–230.
- Allan, D.W., Shoaf, J.H., and Halford, D. (1974). *Time and Frequency: Theory and Fundamentals* (Blair, B.E., ed.) NBS (National Bureau of Standards). Monograph 140. U.S. Government Printing Office, Washington, D.C., pp. 151–166.
- Anliker, P., Luthi, H.R., Seelig, W., Steinger, J., Weber, H.P., Leutwyler, S., Schumacher, E., and Woste, L. (1977). 33-W cw dye laser. *IEEE J. Quant. Elect.* **QE-13**, 547–548.
- Balykin, V.I., Ovchinnikov, Yu. B., and Sidorov, A.I. (1987). Single- and double-frequency cw dye laser with active frequency stabilization and electronic spectral scanning. *Sov. J. Quant. Elect.* **17**, 1535–1539.
- Barger, R.L., Sorem, M.S., and Hall, J.L. (1973). Frequency stabilization of a cw dye laser. *Appl. Phys. Lett.* **22**, 573–575.
- Barger, R.L., West, J.B., and English, T.C. (1975). Fast frequency stabilization of a cw dye laser. *Appl. Phys. Lett.* **27**, 31–33.
- Bergquist, J.C., (1989). Private communication.

- Bergquist, J.C., and Burkins, L. (1984). Efficient single mode operation of a cw ring dye laser with a Mach-Zehnder interferometer. *Opt. Comm.* **50**, 379-385.
- Bergquist, J.C., Hemmati, H., and Itano, W.M. (1982). High power second harmonic generation of 257 nm radiation in an external ring cavity. *Opt. Comm.* **43**, 437-442.
- Biraben, F. (1979). Efficacité des systèmes unidirectionnels utilisables dans les lasers en anneau. *Opt. Comm.* **29**, 353-356.
- Biraben, F. (1989). Private communication.
- Biraben, F., and Labastie, P. (1982). Balayage d'un laser a colorant continu monomode sur 150 GHz. *Opt. Comm.* **41**, 49-51.
- Blit, S., Weaver, E.G., Dunning, F.B., and Tittel, F.K. (1977). Generation of tunable continuous-wave ultraviolet radiation from 257 to 320 nm. *Opt. Lett.* **1**, 58-60.
- Blit, S., Weaver, E.G., Rabson, T.A., and Tittel, F.K. (1978). Continuous wave UV radiation tunable from 285 nm to 400 nm by harmonic and sum frequency generation. *Appl. Optics*, **5**, 721-723.
- Bloom, A.L. (1974). Modes of a laser resonator containing tilted birefringent plates. *J. Opt. Soc. Am.* **64**, 447-452.
- Bonarev, B.V., and Kobtsev, S.M. (1986). Calculation and optimization of a birefringent filter for a cw dye laser. *Opt. Spectrosc.* **60**, 501-504.
- Born, M. and Wolf, E. (1964). *Principles of Optics*, 2nd ed. Macmillan, New York, pp. 323-341.
- Cariou, J., and Luc, P. (1980). *Atlas du Spectre d'Absorption de la Molecule de Tellure*. Laboratoire Aime-Cotton C.N.R.S. II, Orsay, France.
- Clark, D.L., Martin, A.G., Dutta, S.B., and Rogers, W.F. (1986). A high resolution computer controlled dye laser system. *Advances in Laser Science-1*. AIP Conf. series 146, Optical Sci. and Eng. subseries 6, (Stwalley, W.C., and Lapp, M., eds.) American Institute of Physics, New York.
- Couillaud, B. (1981). Generation of cw coherent radiation in the near U.V. *J. de Physique*, colloque C8, supplement 12, tome 42, 115-125.
- Couillaud, B., Dabkiewicz, Ph., Bloomfield, L.A., and Hänsch, T.W. (1982). Generation of continuous-wave ultraviolet radiation by sum-frequency mixing in an external ring cavity. *Opt. Lett.* **7**, 265-267.
- Danielmeyer, H.G. (1971). Effects of drift and diffusion of excited states on spatial hole burning and laser oscillations. *J. Appl. Phys.* **42**, 3125-3132.
- DeVoe, R.G., Fabre, C., Jungmann, K., Hoffnagle, J., and Brewer, R.G. (1988). Precision optical-frequency difference measurements. *Phys. Rev. A* **37**, 1802-1805.
- Drever, R.W.P., Hall, J.L., Kowalski, F.V., Hough, J., Ford, G.M., Munley, A.J., and Ward, H. (1983). Laser phase and frequency stabilization using an optical resonator. *Appl. Phys. B* **31**, 97-105.
- Dunn, M.H., and Ferguson, A.I. (1977). Coma compensation in off-axis laser resonators. *Opt. Comm.* **20**, 214-219.
- Elliot, D.S., Roy, R., and Smith, S.J. (1982). Extracavity laser band-shape and bandwidth modification. *Phys. Rev. A* **26**, 12-18.
- Freeman, R.R., Bjorklund, G.C., Economou, N.P., Liao, P.F., and Bjorkholm, J.E. (1978). Generation of cw VUV coherent radiation by four-wave sum frequency mixing in Sr vapor. *Appl. Phys. Lett.* **33**, 739-742.
- Frölich, D., Stein, L., Schröder, H.W., and Welling, H. (1976). Efficient frequency doubling of cw dye laser radiation. *Appl. Phys.* **11**, 97-101.
- Gerstenkorn, S., and Luc, P. (1978). *Atlas du Spectre d'Absorption de la Molecule d'Iode*. Laboratoire Aime Cotton, C.N.R.S. II, Orsay, France.
- Green, J.M., Hohimer, J.P., and Tittel F.K. (1973). Traveling-wave operation of a tunable cw dye laser. *Opt. Comm.* **7**, 349-350.

- Hall, J.L. (1978). Stabilized lasers and precision measurements. *Science* **202**, 147–156.
- Hall, J.L., and Hänsch, T.W. (1984). External dye-laser frequency stabilizer. *Opt. Lett.* **9**, 502–504.
- Hall, J.L., and Lee, S.A. (1976a). Interferometric real-time display of cw dye laser wavelength with sub-doppler accuracy. *Appl. Phys. Lett.* **29**, 367–369.
- Hall, J.L., and Lee, S.A. (1976b). Control techniques for cw dye lasers. In *Tunable Lasers and Applications* (Mooradian, A., Jaeger, T., and Stokseth, P., eds.). Springer-Verlag, Berlin, pp. 361–366.
- Hall, J.L., Zhu, M., Shimizu, F.J., and Shimizu, K. (1988). External frequency stabilization of a commercial dye laser at the Hertz level. *XVI International Quantum Electronics Digest* (Japan Society of Applied Physics, Tokyo, 1988), pp. 4–5.
- Hänsch, T.W. (1976). Spectroscopic applications of tunable lasers. In *Tunable Lasers and Applications*. (Mooradian, A., Jaeger, T., and Stokseth, P., eds.), Springer-Verlag, Berlin, pp. 326–339.
- Hänsch, T.W., and Couillaud, B. (1980). Laser frequency stabilization by polarization spectroscopy of a reflecting reference cavity. *Opt. Comm.* **35**, 441–444.
- Harri, H.-P., Leutwyler, S., and Schumacher, E. (1982). Nozzle design yielding interferometrically flat fluid jets for use in single-mode dye lasers. *Rev. Sci. Instrum.* **53**, 1855–1858.
- Helmcke, J., Lee, S.A., and Hall, J.L. (1982). Dye laser spectrometer for ultrahigh spectral resolution: Design and performance. *Appl. Opt.* **21**, 1686–1694.
- Helmcke, J., Snyder, J.J., Morinaga, A., Mensing, F., and Glaser, M. (1987). New ultra-high resolution dye laser spectrometer utilizing a non-tunable reference resonator. *Appl. Phys. B* **43**, 85–91.
- Hemmati, H., Bergquist, J.C., and Itano, W.M. (1983). Generation of continuous-wave 194-nm radiation by sum-frequency mixing in an external ring cavity. *Opt. Lett.* **8**, 73–75, and Hemmati, H., and Bergquist, J.C. (1983). Generation of continuous-wave 243-nm radiation by sum-frequency mixing. *Opt. Comm.* **47**, 157–160, and Wineland, D.J., Itano, W.M., Bergquist, J.C., Bollinger, J.J., and Prestage, J.D. (1985). In *Spectroscopy of stored atomic ions*. *Atomic Physics 9*, (Vandyck Jr., J.S., and Fortson, E.N., eds.). World Scientific, Singapore.
- Hills, D., and Hall, J.L. (1989). Ultra stable cavity-stabilized lasers with subhertz linewidth. In *4th Symposium on Frequency Standards and Metrology*, Ancona, Italy, Sept. 1988) De Marchi, A. ed.). Springer-Verlag, Heidelberg.
- Holberg, L.W. (1984). Measurement of the Atomic Energy Level Shift Induced by Blackbody Radiation. Thesis. U. of Colorado, Boulder.
- Hough, J., Hils, D., Rayman, M.D., Ma, L.s., Hollberg, L., and Hall, J.L. (1984). Dye-laser frequency stabilization using optical resonators. *Appl. Phys. B* **33**, 179–185.
- Jarrett, S.M., and Young, J.F. (1979). High-efficiency single-frequency cw ring dye laser. *Opt. Lett.* **4**, 176–178.
- Jenkins, F.A., and White, H.E. (1957). *Fundamentals of Optics*, 3rd ed. McGraw-Hill, New York, p. 565.
- Johnston, T. (1988). High power single frequency operation of dyes over the spectrum from 364 nm to 524 nm pumped by an ultraviolet argon ion laser. *Opt. Comm.* **69**, 147–152.
- Johnston, T.F., Jr. (1987). Tunable dye lasers. In *Encyclopedia of Physical Science and Technology* **14**, Academic Press, Orlando, Fla., pp. 96–141.
- Johnston, T.F., JR., and Proffitt, W. (1980). Design and performance of a broad-band optical diode to enforce one-direction traveling-wave operation of a ring laser. *IEEE J. Quant. Elect.* **QE-16**, 483–488.
- Johnston, T.F. Jr., Brady, R.H., and Proffitt, W. (1982). Powerful single-frequency ring dye laser spanning the visible spectrum. *Appl. Phys.* **21**, 2307–2316.

- Johnston, W.D., Jr., and Runge, P.K. (1972). An improved astigmatically compensated resonator for cw dye laser. *IEEE J. Quant. Elect.* **QE-8** (Corresp.), 724-725.
- Juncar, P., and Pinard, J. (1975). A new method for frequency calibration and control of a laser. *Opt. Comm.* **14**, 438-441.
- Kikuchi, K., and Okoshi, T. (1985). Dependence of semiconductor laser linewidth on measurement time: Evidence of predominance of $1/f$ noise. *Electron. Lett.* **21**, 1011-1012.
- Kogelnik, H.W., Ippen, E.P., Dienes, A., and Shank, C.V. (1972). Astigmatically compensated cavities for cw dye lasers. *IEEE J. Quant. Elect.* **QE-8**, 373-379.
- Kowalski, F.V., Hawkins, R.T., and Schawlow, A.L. (1976). Digital wavemeter for cw lasers. *J. Opt. Soc. Am.* **66**, 965-966.
- Kowalski, F.V., Teets, R.E., Demtroder, W., and Schawlow, A.L. (1978). An improved wavemeter for cw lasers. *J. Opt. Soc. Am.* **68**, 1611-1613.
- Kuhlke, D., Dietel, W. (1977). Mode selection in cw laser with homogeneously broadened gain. *Opt. Quant. Elect.* **9**, 305-313.
- Lee, J.H., Kim, K.C., and Kim K.H. (1988). Threshold pump power of a solar-pumped dye laser. *Appl. Phys. Lett.* **53**, 2021-2022.
- Lieberman, S., and Pinard, J. (1973). Single-mode cw dye laser with large frequency range tunability. *Appl. Phys. Lett.* **24**, 142-144.
- Lichten, W. (1985). Precise wavelength measurements and optical phase shifts. I. general theory. *J. Opt. Soc. Am. A* **2**, 1869-1876.
- Lichten, W. (1986). Precise wavelength measurements and optical phase shifts II. Applications. *J. Opt. Soc. Am. A* **3**, 909-915.
- Loudon, R. (1983). *The Quantum Theory of Light*, 2nd ed. Clarendon Press, Oxford, England.
- Marowsky, G., and Zaraga, F. (1974). A comparative study of dye prism ring lasers. *IEEE J. Quant. Elect.* **QE-10**, 832-837.
- Marshall, C.M., Stickel, R.E., Dunning, F.B., and Tittel, F.K. (1980). Computer controlled intracavity SHG in cw ring dye laser. *Appl. Optics* **19**, 1980-1983.
- Mollenauer, L.F. (1985). Color center lasers. In *Laser Handbook*, vol. 4 (Stitch, M.L., and Bass, M., eds.). North-Holland, Amsterdam, pp. 143-228.
- Mollenauer, L.F., and White, J.C. (1987). General principles and some common features. In *Tunable Lasers* (Mollenauer, L.F., and White, J.C., eds.). Springer-Verlag, Berlin, Heidelberg, pp. 1-18.
- Nieuwesteeg, K.J.B.M., Hollander, Tj., and Alkemade, C.Th.J. (1986). Spectral properties of an Ar-ion laser-pumped tunable cw dye laser. *Opt. Comm.* **59**, 285-289.
- Oka, T. (1988). Report of IR difference frequency generation in the 2 to 5 μm range using the crystal lithium iodate and the method developed by Pine (1974). Presentation at the conference, Coherent Sources for Frontier Spectroscopy, International Center for Theoretical Physics, Aug. 1988, Trieste, Italy.
- Okoshi, T., Kikuchi, K., and Nakayama, A. (1980). Novel method for high resolution measurement of laser output spectrum. *Electron. Lett.* **16**, 630-631.
- Peterson, O.G. (1979). Dye lasers. In *Quantum Electronics, part A. Methods of Experimental Physics*, **15**, (Tang, C.L., ed.). Academic Press, New York, pp. 251-359.
- Peterson, O.B., Tuccio, S.A., and Snavely, B.B. (1970). Cw operation of an organic dye solution laser. *Appl. Phys. Lett.* **17**, 245-247.
- Peterson, O.G., Webb, J.P., McColgin, W.C., and Eberly, J.H. (1971). Organic dye laser threshold. *J. Appl. Phys.* **42**, 1917-1928.
- Pike, C.T. (1974). Spatial hole burning in cw dye lasers. *Opt. Comm.* **10**, 14-17.
- Pine, A.S. (1974). Doppler-limited molecular spectroscopy by difference-frequency mixing. *J. Opt. Soc. Am.* **64**, 1683-1690.

- Pine, A.S. (1976). High-resolution methane ν_3 -band spectra using a stabilized tunable difference-frequency laser system. *J. Opt. Soc. Am.* **66**, 97–108.
- Runge, P.K., and Rosenberg, R. (1972). Unconfined flowing-dye films for cw dye lasers. *IEEE J. Quant. Elect.* **QE-8**, 910–911.
- Salomon, Ch., Hils, D., and Hall, J.L. (1988). Laser stabilization at the millihertz level. *J. Opt. Soc. Am. B* **5**, 1576–1587.
- Sargent, M., Scully, M.O., and Lamb, W.E. (1974). *Laser Physics*. Addison-Wesley, London.
- Schäfer, F.P. (1977). *Dye Lasers, 2nd ed. Vol. 1* of Topics in Applied Physics. Springer-Verlag, Berlin, Heidelberg. (Good summary of dye lasers as of 1977.)
- Schäfer, F.P., Schmidt, W., and Volze, J. (1966). Organic dye solution laser. *Appl. Phys. Lett.* **9**, 306–309.
- Scheerer, L.D., Leduc, M., Vivien, D., Lejus, A.M., and Thery, J. (1986). LNA: A new cw Nd laser tunable around 1.05 and 1.08 μm . *IEEE J. Quant. Elect.* **QE-22**, 713–717.
- Schmidt, W., and Schäfer, F.P. (1967). Blitzlampengepumpte farbstofflaser. *Z. Naturforschg.* **22a**, 1563–1566.
- Schröder, H.W., Welling, H., and Wellegehausen, B. (1973). A narrowband single-mode dye laser. *Appl. Phys.* **1**, 343–348.
- Schröder, H.W., Dux, H., and Welling, H. (1975). Single mode operation of cw dye lasers. *Appl. Phys.* **7**, 21–28.
- Schröder, H.W., Stein, L., Frölich, D., Fugger, B., and Welling, H. (1977). A high-power single-mode cw dye ring laser. *Appl. Phys.*, **14**, 377–380.
- Schulz, P.A. (1988). Single-frequency Ti:Al₂O₃ ring laser. *IEEE J. Quant. Elect.* **24**, 1039–1044.
- Shank, C.V. (1975). Physics of dye lasers. *Rev. Mod. Phys.* **47**, 649–657.
- Siegman, A.E. (1986). *Lasers*. University Science Books, Mill Valley, Calif.
- Smith, P.W. (1972). Mode Selection in Lasers. *Proc. IEEE* **60**, 422–440.
- Snavely, B.B. (1977). Continuous-wave dye lasers. In *Dye Lasers, vol. 1*, 2nd ed. Topics in Applied Physics (Schäfer, F.P., ed.). Springer-Verlag, Berlin, Heidelberg, pp. 86–120.
- Snavely, B.B., and Schäfer, F.P. (1969). Feasibility of CW Operation of dye-lasers. *Phys. Lett.* **28A**, 728–729.
- Snyder, J.J. (1980). Algorithm for fast digital analysis of interference fringes. *Appl. Opt.* **19**, 1223–1225.
- Soffer, B.H., and McFarland, B.B. (1967). Continuously tunable, narrow-band organic dye lasers. *Appl. Phys. Lett.* **10**, 266–267.
- Sorokin, P.P., and Lankard, J.R. (1966). Stimulated emission observed from an organic dye, chloro-aluminum phthalocyanine. *IBM J. Res. Dev.* **10**, 162–163.
- Sorokin, P.P., and Lankard, J.R. (1967). Flashlamp excitation of organic dye lasers: A short communication. *IBM J. Res. Dev.* **11**, 148.
- Spaeth, M., and Bortfeld, D.P. (1966). Stimulated emission from polymethine dyes. *Appl. Phys. Lett.* **9**, 179–181.
- “Squeezed States” (1987). *J. Opt. Am. B* **4** (10), whole issue, and *J. Mod. Optics* **34** (6, 7), whole issue.
- Stepanov, B.I., Rubinov, A.N., and Mostovnikov, V.A. (1967). Optic generation in solutions of complex molecules. *JETP Lett.* **5**, 117–119.
- Tang, C.L., Statz, H., and deMars, G. (1963). Regular spiking and single-mode operation of ruby laser. *Appl. Phys. Lett.* **2**, 222–224. And Tang, C.L., Statz, H., and de Mars, G. (1963). Spectral output and spiking behavior of solid state lasers. *J. Appl. Phys.* **34**, 2289–2295.
- Thiel, E., Zander, C., and Drexhage, K.H. (1986). Continuous wave dye laser pumped by a HeNe laser. *Opt. Comm.* **60**, 396–398.

- Theil, E., Zander, C., and Drexhage, K.H. (1987). Incoherently pumped continuous wave dye laser. *Opt. Comm.* **62**, 171–173.
- Tuccio, S.A., and Strome, F.C., Jr. (1972). Design and operation of a tunable continuous dye laser. *Appl. Optics* **11**, 64–73.
- Williams, G.H., Hobart, J.L., and Johnston, T.F., Jr. (1983). A 10-THz scan range dye laser, with 0.5-MHz resolution and integral wavelength readout. In *Laser Spectroscopy VI* (Weber, H.P., and Luthy, W., eds.). Springer-Verlag, Heidelberg, pp. 422–423.
- Wineland, D.J., Berquist, J.C., Bolinger, J.J., Itano, W.M., Gilbert, S.L., and Hulet, R.G. (1989). Quantum jumps, ion crystals and solid plasmas. CLEO/QELS conference plenary session JA2, Baltimore, Md., unpublished.
- Woods, P.T., Shotton, K.C., and Rowley, W.R.C. (1978). Frequency determination of visible laser light by interferometric comparison with upconverted CO₂ laser radiation. *Appl. Opt.* **17**, 1048–1054.
- Wu, F.Y., Grove, R.E., and Ezekial, S. (1974). Cw dye laser for ultrahigh-resolution spectroscopy. *Appl. Phys. Lett.* **25**, 73–75.
- Yariv, A. (1975). *Quantum Electronics*, 2nd ed. Wiley, New York.